SINGLE EXPONENTIAL APPROXIMATION OF FOURIER TRANSFORMS

by

Patrick McLean, B.Sc. Hons (Tas)

Submitted in fulfilment of the requirements

for the Degree of Doctor of Philosophy

School of Mathematics and Physics
University of Tasmania
August, 2006

I declare that this thesis contains no material which has been accepted for a degree or diploma by the University or any other institution, except by way of background information and duly acknowledged in the thesis, and that, to the best of my knowledge and belief, this thesis contains no material previously published or written by another person, except where due acknowledgement is made in the text of the thesis.

Signed: P. McL

Patrick McLean

Date: 13/9/06

Signed: P. McL

Patrick McLean

Date: 13/9/06

ABSTRACT

This thesis is primarily concerned with a new method for the approximate evaluation of Fourier sine and cosine transforms.

A problem of linear surface waves, discussed by Forbes, initially gave rise to a singular integrodifferential equation over the real line. We have been able to transform this integrodifferential equation into a linear second order differential equation. The solution of this differential equation has been found explicitly in terms of Fourier sine and cosine transforms of simple rational functions. However, the integrands of these integrals decay algebraically rather than exponentially and this leads to problems with their approximate evaluation. This is what has motivated the major part of this thesis.

A commonly used technique of quadrature involves transforming the integral to one over the entire real line and then using the trapezoidal rule in order to approximate the transformed integral. These methods are characterised as to whether the transformed integrand has single exponential decay or double exponential decay.

After a discussion of the literature, we have developed and analysed a new quadrature rule for Fourier sine and cosine transforms. A complete error analysis is made using contour integration and several examples are examined in detail. In particular, we consider an open problem posed by Ooura and Mori. The method we have developed is characterised by its simplicity. We conclude by considering again the linear surface waves problem.

ACKNOWLEDGEMENTS

Thanks to all the people who have helped me complete this thesis. Thanks to David Elliott, Larry Forbes, Simon Wotherspoon, Paola Petrelli.

Contents

1 Introduction **4**

1.1 Background 4

1.2 Thesis Outline 6

1.3 New Results 8

2 Linear Surface Waves **10**

2.1 Derivation of an Integrodifferential Equation 10

2.2 Conversion to a Differential Equation 16

2.3 Behaviour of the Solution 18

3 Exponential Quadrature based on the Trapezoidal Rule **22**

3.1 The Trapezoidal Rule 23

3.2 The Midpoint Rule 24

3.3 Double Exponential Methods versus Single Exponential Methods 25

3.3.1 Half Infinite Interval 26

3.3.2 Example 27

4 Fourier Transforms and their Approximation **34**

4.1 Occurrence of Fourier Transforms 35

4.1.1 Fourier sine and cosine transforms 35

4.1.2 Fourier transforms in applied mathematics 35

4.2 Fourier transforms of rational functions 37

4.3 Miscellaneous Quadrature Methods 38
4.3.1 Filon's Method 39
4.3.2 Lund's Method 39
4.4 Exponentially Convergent Quadrature Methods For Fourier Transforms . . . 41
4.5 Ooura and Mori's two double exponential transformations 42

5 Single Exponential Approximation of Fourier Transforms 45
5.1 Single Exponential Transformation I 47
5.2 Application of our method to the Cosine Integral 48
5.3 Discretisation error 49
5.3.1 Contribution to the error from the poles 50
5.3.2 Alternative derivation of asymptotic behaviour of image of pole . . . 53
5.3.3 Saddle Point Approximation according to de Bruijn 54
5.3.4 Contribution to the error from the saddle points 55
5.3.5 Discussion 58
5.4 Truncation error 61
5.5 Comparison between our method and the method of Ooura and Mori 63
5.6 Reflection of pole about imaginary axis 65
5.7 New Problems 66
5.7.1 A new problem 66
5.7.2 A new hard problem 67
5.8 Single Exponential Transformation II 68

6 Linear Surface Waves II 70
6.1 Alternative Methods Of Solution 71
6.1.1 Domain Truncation 71
6.2 Approximate evaluation of S_0 and C_1 72
6.2.1 Use of Symmetry 73
6.2.2 Approximation to u 73

6.3 Linearised Surface Profile 74

Chapter 1

Introduction

1.1 Background

Fourier transforms are widely used in many fields of science, for example in signal processing and engineering. As an example of their occurrence we consider Fourier transforms of simple rational functions occurring in a free surface problem of fluid mechanics. While there exist many theoretical tools for the evaluation, manipulation and inversion of Fourier transforms there is also a need to approximate them numerically; see, for example, Bracewell [5].

In this thesis we develop a new method for the numerical evaluation of Fourier transforms. Our method is characterised by its exponential convergence and simple nature, making it suitable for efficient, high-accuracy evaluation of Fourier transforms.

It is well known that the numerical evaluation of Fourier transforms is problematic due both to the infinite interval of integration and the oscillatory nature of the integrand, see Davis and Rabinowitz [8]. The existence of singularities of the integrand on or near the interval of integration and its slow decay pose further difficulties. Our analysis highlights the role of the singularities of the integrand in determining the convergence rate of the quadrature error.

We note that the proximity of singularities to the interval of integration determines the rate of convergence. Furthermore, we propose a simple remedy, applicable to certain integrals, that improves the rate of convergence of such methods. This provides an answer to an open problem of Ooura and Mori [21].

Ooura and Mori [20] and [21] have developed an ingenious method for the numerical approximation of Fourier transforms. Their method is based on the evaluation of the integrand at points close to its zeros. In fact, their method samples the integrand at points which are exponentially asymptotic to its zeros. This allows their method to achieve high accuracy using relatively few points compared with classical methods. It is common to quote the asymptotic behaviour of the error of quadrature methods in terms of the number n of function evaluations. In fact, the convergence of their method is exponential, $\exp(-\alpha n/\log(n))$ as n increases without bound. This compares favourably with the algebraic $1/n^{\beta}$ convergence of Filon's method [12] or of Lund's method [15]. Furthermore, their method allows the approximate evaluation of Fourier transforms of functions which are of slow decay. Our method shares these features but converges exponentially $\exp(-\alpha\sqrt{n})$ as n increases without bound.

Ooura and Mori's method [20] is flawed by the fact that while it converges exponentially for some entire functions it is not even convergent for certain meromorphic functions. Subsequently they improved upon that method by introducing a new transformation [21]. This transformation seems unnecessarily complicated. We have developed a method similar to theirs, but our method trades higher asymptotic convergence rate for greater simplicity. Their method relies on cumbersome asymptotic expressions for the location of poles and hence, for the error rate. In contrast, our method allows exact representation of the location of poles and highly accurate error estimates in certain cases. Furthermore, their method requires extra effort in the computation of weights and nodes. We shall see that while their method is better asymptotically than ours, our method is competitive for moderate n.

Our analysis is based on a contour integral representation of the error. We decompose the error into a contribution from the poles of the integrand and a remainder. We show that, for certain meromorphic functions, the error is not represented totally by the residues at the poles. However, we estimate the remainder using the saddle point method and show that it is not always negligible. The location of the saddle points (and hence the determination of their contribution) relies on the solution of a transcendental equation. We demonstrate by considering an example, that our method converges at the exponential rate, $\exp(-\alpha\sqrt{n})$.

We propose another single exponential transformation with similar properties. We do not pursue a detailed analysis of this transformation, instead we compare it numerically to our first transformation.

1.2 Thesis Outline

This thesis is primarily concerned with the numerical approximation of Fourier transforms. We develop and analyse an exponentially convergent method applicable to Fourier transforms of a wide variety of functions.

In Chapter 2, we present the particular problem of a fluid flowing over a disturbance. We derive its solution in terms of Fourier transforms. This situation has previously been studied by Forbes [13, 14]. Modelling of the physical situation results in the integrodifferential equation

$$u + F^2 H u' = f, \qquad u(-\infty) = 0, \tag{1.1}$$

over $\mathbb{R}$. In this equation, H denotes the Hilbert transform, f is a particular rational function and F denotes a parameter known as the Froude number. This problem is converted to a linear second order differential equation which can be readily integrated. We express the solution in terms of Fourier transforms as

$$u(x) = \frac{1}{\pi F^2}\left[\int_0^\infty \frac{\sin(\frac{s}{F^2})}{(s-x)^2+1}\,ds + \int_0^\infty \frac{(s-x)\cos(\frac{s}{F^2})}{(s-x)^2+1}\,ds\right], \tag{1.2}$$

where $x \in \mathbb{R}$.

Thus, we are led to consider the numerical evaluation of integrals of the form

$$\int_0^\infty f(x)\sin(tx)\,dx, \qquad \int_0^\infty f(x)\cos(tx)\,dx, \tag{1.3}$$

for $t \geq 0$, which are known as the Fourier sine and cosine transforms of f, respectively.

Chapter 3 deals with quadrature methods for integrals

$$I = \int_a^b f(x)\,dx. \tag{1.4}$$

The methods we consider are defined by transforming, via a change of variable, the integral to one over $\mathbb{R}$ and then applying the trapezoidal rule, with stepsize h, to give T_h. The infinite sum T_h is truncated to a finite sum $T_{n,h}$ to give an approximation to I. The overall error $I - T_{n,h}$ consists of two parts, the discretisation error $I - T_h$ and the truncation error $T_h - T_{n,h}$. The discretisation error can be represented as a contour integral, while the truncation error relies on the rate of decay of the transformed integrand. Based on estimates for these two components of the error the dependence of h on n is chosen in order to ensure exponential convergence. We present an example highlighting the differences between the double exponential methods of Takahasi and Mori [23] and the single exponential methods of Stenger [22]. We also introduce the midpoint rule for use with Fourier cosine transforms.

The numerical approximation of Fourier transforms requires special attention because of the infinite interval and oscillatory nature of the integrand. Slow decay of $f(x)$ as $x \to \infty$ and the presence of singularities of f may further hinder the accurate evaluation of its Fourier sine or cosine transforms.

The methods of Chapter 3 have been used with great success for non-oscillatory functions while the oscillatory case seems not to have a satisfactory solution. In Chapter 4 we detail these unsatisfactory methods. Lund [15] uses the transformation $x = \sinh^{-1}(e^u)$ followed by the trapezoidal rule. This works well when $f(x)$ has exponential decay, but the Euler transform is required to speed the convergence in the case of algebraic decay. He provides criteria which are not very useful for estimating the error or determining when the method is applicable.

Ooura and Mori [20, 21] introduce novel transformations that actually depend on the stepsize. An ingenious technique allows the infinite trapezoidal sum to be truncated in a way to balance the exponential convergence of the discretisation error.

They estimate the discretisation error using a contour integral representation and we present their estimates in two special cases. They have not published details as to how these results are derived. Their transformation is complicated, their analysis is cumbersome and obscures the important sources of error.

In Chapter 5 we present a new method which uses a variable transformation similar to those of Ooura and Mori in the way it handles the truncation error. We analyse the discretisation and truncation errors and compare our method with those of Ooura and Mori. Our analysis is based on residues and the saddle point method.

In Chapter 6 we return to the linear surface waves problem of Chapter 2 and we also evaluate u using our new method developed in Chapter 5. Finally we present the surface profile for a range of F.

Throughout this thesis we shall let C, α denote generic constants whose value may vary from line to line. Furthermore, we use the symbols $\sim$, o and O according to their definition in Olver [19, pages 4-6]. We include these definitions here for completeness. Given $a \in \mathbb{R}$ or $a = \pm\infty$ we write $f(x) \sim g(x)$ as $x \to a$ if

$$\lim_{x \to a} \frac{f(x)}{g(x)} = 1, \tag{1.5}$$

$f(x) = o(g(x))$ as $x \to a$ if

$$\lim_{x \to a} \frac{f(x)}{g(x)} = 0, \tag{1.6}$$

or $f(x) = O(g(x))$ as $x \to a$ if

$$\lim_{x \to a} \frac{f(x)}{g(x)}, \tag{1.7}$$

exists and is finite.

1.3 New Results

In Section 2.2 we convert the singular integrodifferential equation to a linear second order differential equation and in Section 2.3 we derive some characteristics of the solution using more simple means than those previously used. In Section 6.2 we approximate u using our new method.

We have presented two new single exponential transformations for the numerical integration of Fourier transforms (see Sections 5.1 and 5.8). We have investigated one of these transformations in detail (see Sections 5.2-5.4). The simple form of our transformation allows a representation of discretisation error in terms of residues in certain cases. We have made use of the saddle point method to estimate the error not represented by the residues at the poles.

While our transformations produce asymptotically slower convergence than those of Ooura and Mori, for moderate values of n the two methods produce similar errors (see Section 5.5) . Furthermore, our method has a lower overhead for the computation of weights and nodes than the methods of Ooura and Mori.

In Section 5.7 we present a solution to an open problem of Ooura and Mori, see equation (4.15) of [21]. In Section 5.6 we present two functions as examples of functions which are difficult to approximate with a high rate of exponential convergence.

This thesis has two occurrences of the Lambert W function. These occurrences are incidental but nonetheless of interest (see Sections 4.1.2 and 5.8).

Chapter 2

Linear Surface Waves

In this chapter we describe a mathematical model of fluid flow over a disturbance. This problem motivates the development of our new method for the numerical approximation of Fourier transforms, which forms the core of this thesis.

In Section 2.1 we present the derivation of an integrodifferential equation which models the surface of the fluid. This derivation is well known and we follow the presentation of Forbes [13, 14]. In Section 2.2 we recast this integrodifferential equation as a differential equation. We are able to integrate this differential equation and obtain an analytic solution u in terms of Fourier transforms of rational functions. In Section 2.3 we determine the asymptotic behaviour of u and the behaviour at the origin of the solution $\hat{u}$.

We shall return to this problem in the last chapter where we employ the approximation methods of Chapter 5 to present a graphical representation of the surface for a range of Froude numbers F.

2.1 Derivation of an Integrodifferential Equation

We consider the situation of a fluid flowing over a vortex. It is expected that the presence of the vortex will produce a stationary wave downstream. It will be seen that this is indeed the case.

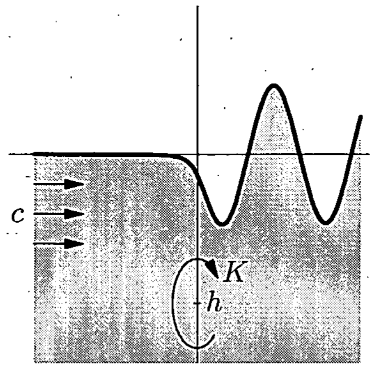

Figure 2.1: The physical situation - An infinitely deep ideal fluid flowing steadily over a vortex produces waves downstream

The derivation presented here closely follows Forbes [14]. Consider a fluid flowing over a (line) vortex. The fluid is assumed to be ideal, that is, it is inviscid, incompressible and irrotational. The fluid is assumed to be of infinite depth and flowing with constant velocity far upstream. In particular, let the fluid be flowing with upstream velocity c and let the vortex be of strength K at depth h. We denote the acceleration due to gravity as g. This physical situation is displayed in Figure 2.1.

In order to nondimensionalise the problem we introduce characteristic length h and characteristic speed c. The Froude number is a dimensionless parameter and is defined by

$$F = \frac{c}{\sqrt{gh}}. \tag{2.1}$$

We shall see that F controls the shape of the free surface. The dimensionless vortex strength is defined by

$$\epsilon = \frac{K}{ch}, \tag{2.2}$$

and we shall see that ϵ determines the asymptotic wave height. The nondimensionalised situation is displayed in Figure 2.2.

Taking a vertical cross-section of the fluid we shall describe the flow in terms of an analytic function satisfying nonlinear boundary conditions at the surface which itself is unknown.

In particular, we seek a complex potential $\Phi(z)$ and surface profile $y = S(x)$. We denote the real and imaginary parts of $\Phi(z)$ by $\phi(x,y)$ and $\psi(x,y)$ respectively, where $z = x + iy$. We require $\Phi(z)$ to be analytic in the region of the complex plane described by

$$\{z = x + iy \in \mathbb{C} | y < S(x)\} \setminus \{-i\}. \tag{2.3}$$

We require $\Phi(z)$ to behave like a constant flow superimposed upon a vortex as $z \to -i$, that is, we impose the condition that

$$\Phi(z) \to z + \frac{i\epsilon}{2\pi} \log(z + i), \tag{2.4}$$

as $z \to -i$. We require that upstream the flow is uniform with velocity 1, that is, we impose the radiation condition

$$\Phi(z) \to z, \tag{2.5}$$

as $\Re z \to -\infty$. At the surface $y = S(x)$, we impose the free surface condition (see Forbes [13, eqn 2.4])

$$\phi_x S' = \phi_y, \tag{2.6}$$

together with Bernoulli's equation (see Forbes [13, eqn 2.5])

$$\frac{1}{2}F^2\left(\phi_x^2 + \phi_y^2\right) + y = \frac{1}{2}F^2. \tag{2.7}$$

Together, equations (2.4) - (2.7) describe a nonlinear free-surface problem.

Based on the assumption that ϵ is of small magnitude we make perturbation expansions of $\Phi(z)$ and $S(x)$; we write

$$\begin{aligned} \Phi(z) &= z + \epsilon\Phi_1(z) + O(\epsilon^2), & (2.8)\\ S(x) &= \epsilon S_1(x) + O(\epsilon^2). & (2.9) \end{aligned}$$

This results in a linear problem for $\Phi_1(z) = \phi_1 + i\psi_1$, where ϕ_1 and ψ_1 are the real and imaginary parts of Φ_1.

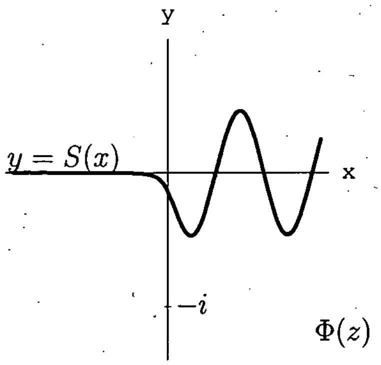

Figure 2.2: The nondimensionalised physical situation modelled as a nonlinear free-surface problem

Now, $\Phi_1(z)$ is analytic in the lower half plane (except at $z = -i$) and the following conditions follow from equations (2.4) - (2.7):

$$\Phi_1(z) \longrightarrow \frac{i}{2\pi}\log(z+i), \quad \text{as} \quad z \longrightarrow -i \tag{2.10}$$

$$\Phi_1(z) \longrightarrow 0, \quad \text{as} \quad \Re z \longrightarrow -\infty \tag{2.11}$$

$$S_1' = \frac{\partial \phi_1}{\partial y}, \quad \text{on} \quad y = 0 \tag{2.12}$$

$$F^2\frac{\partial \phi_1}{\partial x} + S_1 = 0, \quad \text{on} \quad y = 0. \tag{2.13}$$

From these four equations we shall derive an integrodifferential equation for $\frac{\partial \phi_1}{\partial x}(x,0)$. In order to achieve this we introduce the function G defined by

$$G(z) = \frac{d}{dz}\left(\Phi_1(z) - \frac{i}{2\pi}\left[\log(z+i) - \log(z-i)\right]\right). \tag{2.14}$$

It follows from (2.10) that G is analytic in the lower half plane. A simple calculation gives

$$G(z) = \Phi_1'(z) - \frac{1}{\pi}\frac{1}{z^2+1}. \tag{2.15}$$

Now consider $x_0 \in \mathbb{R}$ and positive numbers ϵ, R such that ϵ is small with respect to R.

Define the contour C_R to be the semicircular arc of radius R and centre 0. Define the contour C_ϵ to be the semicircular arc of radius ϵ and centre x_0. Join C_R and C_ϵ by the intervals $(-R, x_0 - \epsilon)$ and $(x_0 + \epsilon, R)$ to create the closed contour $C_{R,\epsilon}$. Orient $C_{R,\epsilon}$ in the positive sense as depicted in Figure 2.3. Let C_R and C_ϵ take their orientation from $C_{R,\epsilon}$.

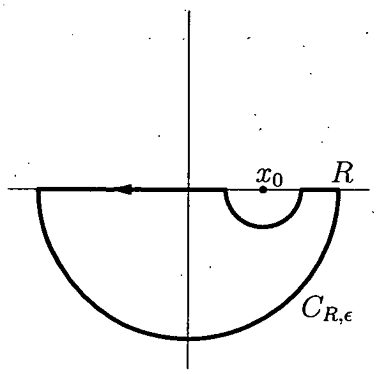

Figure 2.3: The contour $C_{R,\epsilon}$. We use the boundary integral method to obtain an integrodifferential equation.

Now, since G is analytic inside $C_{R,\epsilon}$, we have by Cauchy's formula that

$$\frac{1}{2\pi i}\int_{C_{R,\epsilon}} \frac{G(z)}{z-x_0}\,dz = 0, \tag{2.16}$$

where $x_0 \in \mathbb{R}$. On taking limits $\epsilon \to 0+$ and $R \to \infty$ this becomes

$$\lim_{\epsilon\to 0+, R\to\infty} \frac{1}{2\pi i}\left(-\int_{-R}^{x_0-\epsilon} + \int_{C_R} - \int_{x_0+\epsilon}^{R} + \int_{C_\epsilon}\right)\frac{G(z)}{z-x_0}\,dz = 0. \tag{2.17}$$

We assume that the contribution over C_R is negligible as $R \to \infty$, that is,

$$\lim_{R\to\infty} \frac{1}{2\pi i}\int_{C_R} \frac{G(z)}{z-x_0}\,dz = 0. \tag{2.18}$$

Furthermore, a short calculation gives

$$\lim_{\epsilon\to 0+} \frac{1}{2\pi i}\int_{C_\epsilon} \frac{G(z)}{z-x_0}\,dz = -\frac{1}{2}G(x_0). \tag{2.19}$$

Thus, from (2.17) we have that

$$-\frac{1}{2\pi i}⨍_{-\infty}^{\infty} \frac{G(x)}{x-x_0}\,dx - \frac{1}{2}G(x_0) = 0, \tag{2.20}$$

where the integral denotes a Cauchy principal value integral defined by

$$⨍_{-\infty}^{\infty} \frac{G(x)}{x-x_0}\,dx = \lim_{\epsilon\to 0+, R\to\infty}\left(\int_{-R}^{x_0-\epsilon} + \int_{x_0+\epsilon}^{R}\right)\frac{G(x)}{x-x_0}\,dx, \tag{2.21}$$

Substituting the expression (2.15) for G into equation (2.20), we obtain

$$\Phi_1'(x_0) - \frac{1}{\pi}\frac{1}{{x_0}^2+1} = -\frac{1}{\pi i}\fint_{-\infty}^{\infty}\left(\Phi_1'(x) - \frac{1}{\pi}\frac{1}{x^2+1}\right)\frac{dt}{x-x_0}. \tag{2.22}$$

Equating real parts of (2.22) we have that

$$\frac{\partial\phi_1}{\partial x}(x_0,0) - \frac{1}{\pi({x_0}^2+1)} = -\frac{1}{\pi}\fint_{-\infty}^{\infty}\frac{\partial\psi_1}{\partial x}(x,0)\frac{dt}{x-x_0}. \tag{2.23}$$

Now, we need to find $\frac{\partial\psi_1}{\partial x}(x,0)$ in terms of $\frac{\partial\phi_1}{\partial x}(x,0)$. From the Cauchy-Riemann equations it follows that

$$\frac{\partial\psi_1}{\partial x} = -\frac{\partial\phi_1}{\partial y}, \tag{2.24}$$

and, on using (2.12) and (2.13), we have that

$$\begin{aligned}\frac{\partial\psi_1}{\partial x} &= -S_1' \\ &= F^2\frac{\partial^2\phi_1}{\partial x^2}.\end{aligned} \tag{2.25}$$

Using this relation allows us to express equation (2.23) as

$$\frac{\partial\phi_1}{\partial x}(x_0,0) + \frac{F^2}{\pi}\fint_{-\infty}^{\infty}\frac{\partial^2\phi_1}{\partial^2 x}(x,0)\frac{dx}{x-x_0} = \frac{1}{\pi({x_0}^2+1)}, \tag{2.26}$$

where $-\infty < x_0 < \infty$. This equation appears in Forbes [14, eqn 2.8]. From $\phi_1(x,0)$ we can determine $S_1(x)$. In particular, from (2.13) the linearised surface profile is given by

$$S_1(x_0) = -F^2\frac{\partial\phi_1}{\partial x}(x_0,0), \tag{2.27}$$

for $-\infty < x_0 < \infty$.

We follow Erdélyi [11, §15.1] and define the Hilbert transform of a function g to be

$$Hg(x_0) = \frac{1}{\pi}\fint_{-\infty}^{\infty}\frac{g(x)}{x-x_0}dx, \tag{2.28}$$

where the integral is taken in the Cauchy principal value sense given by (2.21).

If we introduce the notation

$$u(x) = \frac{\partial\phi_1}{\partial x}(x,0) \tag{2.29}$$

$$f(x) = \frac{1}{\pi(x^2+1)}, \tag{2.30}$$

we can express equation (2.26) as

$$u + F^2 Hu' = f. \tag{2.31}$$

This equation is an integrodifferential equation, and to solve it uniquely we need to specify an extra condition. Since, we are seeking a solution to equation (2.31) which vanishes at $-\infty$ we shall impose the boundary condition

$$\lim_{x\to-\infty} u(x) = 0. \tag{2.32}$$

For more background on this derivation, see Forbes [13] and [14].

2.2 Conversion to a Differential Equation

In this section we convert the integrodifferential equation (2.31) to a differential equation. The resulting equation is integrated using the method of variation of parameters to give a representation of u as an integral.

Differentiating (2.31), applying H and multiplying by F^2 gives

$$F^2 Hu' + F^4 H(Hu')' = F^2 Hf'. \tag{2.33}$$

Using the results $H^2 u = -u$, see Erdélyi [11, §15.1 (2)] and $Hu' = (Hu)'$, see Erdélyi [11, §15.1 (8)] we have that $H(Hu')' = -u''$. Thus, (2.33) becomes

$$F^2 Hu' - F^4 u'' = F^2 Hf'. \tag{2.34}$$

Subtracting (2.34) from (2.31) gives the second order differential equation

$$F^4 u'' + u = f - F^2 Hf'. \tag{2.35}$$

The general solution to the homogeneous part of this equation is

$$A\sin(\frac{x}{F^2}) + B\cos(\frac{x}{F^2}) \tag{2.36}$$

for arbitrary constants A and B. By the method of variation of parameters (see for example Boyce and DiPrima [4]), we find that a particular solution u_p, which is zero at $-\infty$, is given by

$$u_p(x) = \frac{1}{F^2}\int_{-\infty}^{x} \sin(\frac{x-s}{F^2})\left[f(s) - F^2 Hf'(s)\right] ds. \tag{2.37}$$

Thus, the general solution of equation (2.35) is given by

$$u(x) = A\sin(\frac{x}{F^2}) + B\cos(\frac{x}{F^2}) + u_p(x). \tag{2.38}$$

Imposing condition (2.32) we have, since $u_p(-\infty) = 0$, that both A and B must be zero. So, the required solution is

$$u(x) = \frac{1}{F^2}\int_{-\infty}^{x} \sin(\frac{x-s}{F^2})\left[f(s) - F^2 Hf'(s)\right] ds. \tag{2.39}$$

Since $Hf' = (Hf)'$ we can apply integration by parts to give

$$\int_{-\infty}^{x} \sin(\frac{x-s}{F^2})(Hf)'(s)ds = \left[\sin(\frac{x-s}{F^2})Hf(s)\right]_{-\infty}^{x} + \frac{1}{F^2}\int_{-\infty}^{x} \cos(\frac{x-s}{F^2})Hf(s)ds. \tag{2.40}$$

The following Hilbert transform is to be found in Erdélyi [11, §15.2 (10)]

$$(Hf)(x) = \frac{1}{\pi}H(\frac{1}{x^2+1}) = \frac{-x}{\pi(x^2+1)}, \tag{2.41}$$

from which we see that

$$\lim_{x\to-\infty} Hf(x) = 0. \tag{2.42}$$

From (2.39), (2.40) and (2.42) we have the representation

$$u(x) = \frac{1}{F^2}\int_{-\infty}^{x} \left[\sin(\frac{x-s}{F^2})f(s) - \cos(\frac{x-s}{F^2})Hf(s)\right] ds. \tag{2.43}$$

Invoking the change of variable $x - s = r$ in equation (2.43) and substituting for f and Hf, from (2.30) and (2.41) respectively, we obtain

$$u(x) = \frac{1}{\pi F^2}\int_{0}^{\infty} \left[\sin(\frac{r}{F^2})\frac{1}{(r-x)^2+1} - \cos(\frac{r}{F^2})\frac{r-x}{(r-x)^2+1}\right] dr. \tag{2.44}$$

For $a \in \mathbb{R}$, $b > 0$ and $t > 0$ define the function $S_0(a, b, t)$ by

$$S_0(a,b,t) = \int_0^\infty \frac{\sin(xt)}{(x-a)^2 + b^2}\, dx, \tag{2.45}$$

and the function $C_1(a, b, t)$ by

$$C_1(a,b,t) = \int_0^\infty \frac{(x-a)\cos(xt)}{(x-a)^2 + b^2}\, dx. \tag{2.46}$$

In which case, from (2.44) we may identify $u(x)$ as the linear combination

$$u(x) = \frac{1}{\pi F^2}(S_0(x, 1, 1/F^2) - C_1(x, 1, 1/F^2)). \tag{2.47}$$

We shall return to this representation of u in Section 6.2 after we have developed, in Chapter 5, a new method for the approximation of such integrals.

2.3 Behaviour of the Solution

In this section we examine the asymptotic behaviour at $+\infty$ of the solution (2.43). Rewrite (2.43) as

$$\begin{aligned} u(x) &= \frac{1}{F^2}\int_{-\infty}^\infty \left[\sin(\frac{x-s}{F^2})f(s) - \cos(\frac{x-s}{F^2})Hf(s)\right] ds \\ &\quad -\frac{1}{F^2}\int_x^\infty \left[\sin(\frac{x-s}{F^2})f(s) - \cos(\frac{x-s}{F^2})Hf(s)\right] ds. \end{aligned} \tag{2.48}$$

The second integral in this representation vanishes as $x \to \infty$, so we have that

$$u(x) \sim \frac{1}{F^2}\int_{-\infty}^\infty \sin(\frac{x-s}{F^2})f(s)ds - \frac{1}{F^2}\int_{-\infty}^\infty \cos(\frac{x-s}{F^2})Hf(s)ds, \tag{2.49}$$

as $x \to \infty$. We shall need the following two properties of the Hilbert transform:

$$\int_{-\infty}^\infty f(x-s)Hg(s)\, ds = \int_{-\infty}^\infty Hf(x-s)g(s)\, ds. \tag{2.50}$$

and

$$H\cos = -\sin, \tag{2.51}$$

which are to be found in Butzer and Nessel [6, eqn 8.2.5] and Erdélyi [11, §15.2 (47)], respectively.

Thus, (2.49) becomes

$$\begin{aligned} u(x) &\sim \frac{1}{F^2}\int_{-\infty}^{\infty}\sin(\frac{x-s}{F^2})f(s)ds - \frac{1}{F^2}\int_{-\infty}^{\infty}H\cos(\frac{x-s}{F^2})f(s)ds \\ &= \frac{2}{F^2}\int_{-\infty}^{\infty}\sin(\frac{x-s}{F^2})f(s)ds, \end{aligned} \tag{2.52}$$

as $x \to \infty$. Now, using the fact that the sine function is odd and f is even (see (2.30)) it follows that

$$u(x) \sim \frac{2}{\pi F^2}\sin(\frac{x}{F^2})\int_{-\infty}^{\infty}\cos(\frac{s}{F^2})\frac{1}{s^2+1}ds, \tag{2.53}$$

as $x \to \infty$. On using the Fourier cosine transform to be found in Erdélyi [11, §1.2 (11)]

$$\int_0^{\infty}\frac{\cos(xt)}{x^2+a^2}dx = \frac{\pi}{2a}e^{-at}, \qquad a, t > 0, \tag{2.54}$$

we obtain

$$u(x) \sim 2\frac{e^{-\frac{1}{F^2}}}{F^2}\sin(\frac{x}{F^2}), \tag{2.55}$$

as $x \to \infty$. From (2.27), (2.29) and (2.9) we see that

$$S(x) = -2\epsilon e^{-\frac{1}{F^2}}\sin(\frac{x}{F^2}) + O(\epsilon^2), \quad x \to \infty. \tag{2.56}$$

This agrees with standard linearised theory as quoted in Forbes [14, eqn 3.4], but our derivation appears to be more straightforward. Thus, we have found the asymptotic behaviour at $+\infty$ of the function u. That is, the solution oscillates sinusoidally at $+\infty$.

We now note the value of u and its derivative at the origin. For $u(0)$ we have from (2.44) that

$$u(0) = \frac{1}{\pi F^2}\int_0^{\infty}\left[\sin(\frac{r}{F^2})\frac{1}{r^2+1} - \cos(\frac{r}{F^2})\frac{r}{r^2+1}\right]dr. \tag{2.57}$$

Differentiating (2.43) we have that

$$u'(x) = \frac{1}{F^2}\left(-Hf(x) + \frac{1}{F^2}\int_{-\infty}^{x}\left[\cos(\frac{x-s}{F^2})f(s) + \sin(\frac{x-s}{F^2})Hf(s)\right]ds\right). \tag{2.58}$$

Now, evaluating this expression at $x = 0$ and using (2.41) we obtain

$$u'(0) = \frac{1}{F^4} \int_{-\infty}^{0} \left[\cos(\frac{s}{F^2}) f(s) - \sin(\frac{s}{F^2}) H f(s) \right] ds. \tag{2.59}$$

Making the change of variable $s = -r$ and again using (2.41) and (2.30), we have that

$$u'(0) = \frac{1}{\pi F^4} \int_{0}^{\infty} \left[\cos(\frac{r}{F^2}) \frac{1}{r^2 + 1} + \sin(\frac{r}{F^2}) \frac{r}{r^2 + 1} \right] dr. \tag{2.60}$$

We shall use the following identity, which can be found in Abramowitz and Stegun [1, eqn 5.1.31],

$$\int_{0}^{\infty} \frac{r + i}{r^2 + 1} e^{irt}\, dr = e^{-t}(-\operatorname{Ei}(t) + i\pi), \tag{2.61}$$

where $t > 0$ and the exponential integral function Ei is defined in Abramowitz and Stegun [1, eqn 5.1.2] as

$$\operatorname{Ei}(x) = -⨍_{-x}^{\infty} \frac{e^{-t}}{t}\, dt, \tag{2.62}$$

for $x > 0$. Taking real and imaginary parts of (2.61) gives

$$\int_{0}^{\infty} \frac{\sin(rt) - r\cos(rt)}{r^2 + 1}\, dr = e^{-t} \operatorname{Ei}(t), \tag{2.63}$$

$$\int_{0}^{\infty} \frac{r\sin(rt) + \cos(rt)}{r^2 + 1}\, dr = \pi e^{-t}. \tag{2.64}$$

Thus, from equation (2.57) we have that

$$u(0) = \frac{e^{-\frac{1}{F^2}}}{\pi F^2} \operatorname{Ei}(\frac{1}{F^2}), \tag{2.65}$$

and from equation (2.60) we have that

$$u'(0) = \frac{e^{-\frac{1}{F^2}}}{F^4}. \tag{2.66}$$

In this chapter we have modelled steady, ideal flow over a vortex. We have derived an equation for the linearised surface and solved this equation in terms of function S_0 and C_1. We have derived expressions for the asymptotic wave height, see (2.56) and behaviour at the origin, see (2.65) and (2.66).

We shall return to this problem in Chapter 6 after efficient methods for the approximate evaluation of S_0 and C_1 are developed in Chapter 5. In Chapter 6 we also consider a method of approximating $u(x)$ based on truncating the differential equation (2.35) to the domain $(-L, L)$ for given $L > 0$.

Chapter 3

Exponential Quadrature based on the Trapezoidal Rule

The modelling problem of the previous chapter resulted in a solution expressible in terms of the Fourier integrals S_0 and C_1, as defined in (2.45) and (2.46), respectively. It is the goal of this thesis to develop quadrature methods for Fourier integrals. In this chapter we discuss, in general, quadrature methods based on the trapezoidal rule.

In Section 3.1, for the Fourier sine integral, we discuss the trapezoidal rule for approximating integrals over the real line. After defining the rule we present a representation of its error in terms of a contour integral. We also discuss the practical implementation of the rule using a finite number of terms. In Section 3.2 we introduce the related midpoint rule which will be used in the approximation of Fourier cosine transforms.

In Section 3.3 we introduce a variation of the trapezoidal rule enabling the approximation of integrals over general intervals (a, b). The trapezoidal rule forms the basis of the single exponential (or Sinc) methods extensively developed by Stenger [22] and also of the double exponential methods developed by Takahasi and Mori [23]. These methods involve mapping the given integral to one over $(-\infty, \infty)$ and then applying the trapezoidal rule. Care must be taken regarding the resulting decay rate of the mapped integrand as this affects the rate of convergence of the method. As a demonstration we take a particular integral over $(0, \infty)$

and present single and double exponential approximations.

3.1 The Trapezoidal Rule

Given a function f defined on $(-\infty, \infty)$ with integral

$$I = \int_{-\infty}^{\infty} f(x)dx, \tag{3.1}$$

and a real number $h > 0$, we define the trapezoidal approximation T_h to I by

$$T_h = h \sum_{k=-\infty}^{\infty} f(kh). \tag{3.2}$$

The trapezoidal rule can be obtained by integrating a piecewise linear interpolant of f. Alternatively, this rule can be developed by integrating a Sinc approximation to f, as is done in the works of Stenger [22].

The error $I - T_h$ is referred to as the *discretisation error.* To estimate $I - T_h$ we use the contour integral error representation of Donaldson and Elliott [10]. From [10, eqn (2.4)] we have the error representation

$$I - T_h = \frac{1}{2\pi i} \int_C \frac{\Psi_h^T(w)}{\Phi_h^T(w)} f(w)\, dw, \tag{3.3}$$

where C is a positively described contour enclosing the real line. The function f must be analytic in a domain containing C and the functions $\Phi_h^T(w)$ and $\Psi_h^T(w)$ are given by

$$\Psi_h^T(w) = \begin{cases} \pi \exp(i\frac{\pi}{h}w), & \Im w > 0 \\ \pi \exp(-i\frac{\pi}{h}w), & \Im w < 0 \end{cases} \tag{3.4}$$

$$\Phi_h^T(w) = -\sin(\frac{\pi}{h}w), \tag{3.5}$$

respectively. These expressions for $\Phi_h^T(w)$ and $\Psi_h^T(w)$ are obtained by setting $\lambda = 0$, $a = 0$ and $\nu = 1/h$ in equations (6.1) and (6.4), respectively, of [10].

In practice, the infinite trapezoidal sum T_h is truncated to give the finite trapezoidal sum $T_{n,h}$:

$$T_{n,h} = h \sum_{k=-n}^{n} f(kh), \tag{3.6}$$

as an approximation to I. This introduces an error $T_h - T_{n,h}$ which we refer to as the *truncation error.*

Thus, the overall error $I - T_{n,h}$ can be written as

$$I - T_{n,h} = (I - T_h) + (T_h - T_{n,h}). \tag{3.7}$$

It is essential that the discretisation error $I - T_h$ and the truncation error $T_h - T_{n,h}$ are of the same order to achieve an optimal rate of convergence. We shall demonstrate this in Section 3.3.

3.2 The Midpoint Rule

Although not commonly used in the definition of single or double exponential quadrature rules, the midpoint rule will be essential in this thesis for the approximation of Fourier cosine transforms. We define the midpoint approximation to I as

$$M_h = h \sum_{k=-\infty}^{\infty} f((k + \frac{1}{2})h). \tag{3.8}$$

To estimate $I - M_h$ we again use the error representation of Donaldson and Elliott [10]. From [10, eqn 2.4] we have the error representation

$$I - M_h = \frac{1}{2\pi i} \int_C \frac{\Psi_h^M(w)}{\Phi_h^M(w)} f(w)\, dw. \tag{3.9}$$

where C is a positively described contour enclosing the real line. The function f must be analytic in a domain containing C and the functions $\Phi_h^M(w)$ and $\Psi_h^M(w)$ are given by

$$\Psi_h^M(w) = \begin{cases} -i\pi \exp(i\frac{\pi}{h}w), & \Im w > 0 \\ i\pi \exp(-i\frac{\pi}{h}w), & \Im w < 0 \end{cases} \tag{3.10}$$

$$\Phi_h^M(w) = \cos(\frac{\pi}{h}w), \tag{3.11}$$

These expressions for $\Phi_h^M(w)$ and $\Psi_h^M(w)$ are obtained by setting $\lambda = 1/2$, $a = 0$ and $\nu = 1/h$ in equations (6.1) and (6.4) of [10].

As for the trapezoidal rule, in practice the infinite midpoint approximation M_h is truncated to give the finite midpoint rule

$$M_{n,h} = h \sum_{k=-n}^{n} f((k+1/2)h). \tag{3.12}$$

Again, it is essential to match the orders of the discretisation error $I - M_h$ and of the truncation error $M_h - M_{n,h}$ in order to achieve a optimal rate of convergence.

3.3 Double Exponential Methods versus Single Exponential Methods

The quadrature methods developed in this thesis involve transforming our integrals (over $(0,\infty)$) to the entire real line and then using the trapezoidal (or midpoint) rule. Such methods have been used widely in the past, for example by Stenger [22] and by Takahasi and Mori [23]. We shall review two families of such techniques - double exponential and single exponential. They are characterised by the decay of the integrand following the transformation. This rate of decay determines the truncation error and, hence, the overall convergence rate of the method.

Given the integral

$$I = \int_a^b f(x)\, dx \tag{3.13}$$

and a suitable transformation $\phi : (-\infty,\infty) \to (a,b)$, we make the change of variable $x = \phi(u)$ and obtain the following representation for I

$$I = \int_{-\infty}^{\infty} f(\phi(u))\phi'(u)\, du. \tag{3.14}$$

This integral is then approximated by the trapezoidal rule (see (3.2))

$$T_h = h \sum_{k=-\infty}^{\infty} f(\phi(kh))\phi'(kh). \tag{3.15}$$

We truncate this infinite sum to give

$$T_{n,h} = h \sum_{k=-n}^{n} f(\phi(kh))\phi'(kh), \tag{3.16}$$

In the next section we present asymptotic estimates for the discretisation error $I - T_h$ and the truncation error $T_h - T_{n,h}$ in terms of h and n. Equating the orders of these estimates allows n and h to be related and allows the method to achieve an optimal rate of convergence.

Furthermore, the truncation error depends on the behaviour of $\phi'(u)$ at $\pm\infty$ together with the behaviour of f near the end points of (a, b). To estimate the discretisation error we shall use the representation (3.3). For rational functions f we shall see that the discretisation error is determined by the proximity of the singularities of f to the interval of integration, when f is considered a function of a complex variable.

3.3.1 Half Infinite Interval

Since the Fourier sine and cosine transforms are defined as integrals over $(0, \infty)$, in this section we consider integrals over this domain. Thus, we shall consider the integral

$$I = \int_0^\infty f(x)\, dx. \tag{3.17}$$

The particular transformations introduced in this chapter are denoted by $\psi_j, j = 1, 2, 3, 4$ while we reserve the notation $\phi_j, j = 1, 2, 3, 4$ for transformations to be introduced in the following chapters.

We shall make the distinction between algebraically decaying integrands such as in the integral

$$\int_0^\infty \frac{\sqrt{x}}{x^2 + 1}\, dx \tag{3.18}$$

where $f(x) = O(1/x^{\frac{3}{2}})$ as $x \to \infty$ and exponentially decaying ones, as in the integral

$$\int_0^\infty \operatorname{sech}(x)\, dx, \tag{3.19}$$

where $f(x) = O(e^{-x})$ as $x \to \infty$.

For algebraically decaying integrands it is suggested (Stenger [22, eqn 4.2.49] or Takahasi and Mori [23, eqn 4.5]) to make the following change of variable

$$x = \psi_1(u) = \exp(u), \tag{3.20}$$

in which case the resulting integrand $f(\psi_1(u))\psi_1'(u)$ decays single exponentially, that is,

$$f(\psi_1(u))\psi_1'(u) = O(\exp(-\alpha|u|)), \tag{3.21}$$

as $u \to \pm\infty$, where α is a positive constant.

To achieve a double exponentially decaying integrand Takahasi and Mori [23, eqn 3.5] instead suggest the transformation

$$x = \psi_2(u) = \exp\left(\frac{\pi}{2}\sinh(u)\right), \tag{3.22}$$

in which case the resulting integrand $f(\psi_2(u))\psi_2'(u)$ decays double exponentially, that is,

$$f(\psi_2(u))\psi_2'(u) = O(\exp(-\alpha\exp(|u|))), \tag{3.23}$$

as $u \to \pm\infty$, where α is a positive constant.

If the function $f(x)$ already decays exponentially, the following change of variable is suggested by Stenger [22, 4.2.56]

$$x = \sinh^{-1}(\exp(u)). \tag{3.24}$$

In the same case, Takahasi and Mori [23, eqn 3.5] suggest making the change of variable

$$x = \exp(u - \exp(-u)), \tag{3.25}$$

in order to achieve a double exponentially decaying integrand.

3.3.2 Example

To illustrate the previous points we shall consider the integral

$$I = \int_0^\infty \frac{1}{(x - x_0)^2 + 1}\, dx = \frac{\pi}{2} + \arctan(x_0), \tag{3.26}$$

Note that in this case the integrand $f(x) = \frac{1}{(x-x_0)^2+1}$ decays algebraically towards ∞. We shall present two methods illustrating each of the techniques - single exponential and double exponential.

We make the change of variable

$$x = \psi_j(u), \qquad j = 1, 2, \tag{3.27}$$

where $\psi_1(u)$ and $\psi_2(u)$ are given by (3.20) and (3.22), respectively, to give the representation

$$I = \int_{-\infty}^{\infty} f(\psi_j(u))\psi_j'(u)\, du. \tag{3.28}$$

Now, approximate I by applying the trapezoidal rule with stepsize $h > 0$ to give the approximation

$$T_h^{(j)} = h \sum_{k=-\infty}^{\infty} f(\psi_j(kh))\psi_j'(kh). \tag{3.29}$$

Truncate this infinite sum to the finite sum

$$T_{n,h}^{(j)} = h \sum_{k=-n}^{n} f(\psi_j(kh))\psi_j'(kh), \tag{3.30}$$

for some positive integer n.

We first consider the discretisation error defined by $I - T_h^{(j)}$. From (3.3) we have that

$$I - T_h^{(j)} = \frac{1}{2\pi i} \int_C \frac{\Psi_h^T(w)}{\Phi_h^T(w)} f(\psi_j(w))\psi_j'(w)\, dw, \tag{3.31}$$

where $\Psi_h^T(w)$ and $\Phi_h^T(w)$ are given by (3.4) and (3.5), respectively, and where C is a positively described contour enclosing the real axis inside which $f(\psi_j(w))\psi_j'(w)$ is analytic. The contour C is depicted in Figure 3.1.

The integrand $f(\psi_j(w))\psi_j'(w)$ has poles $w_j, \overline{w_j}$ which are given as solutions to the equation

$$\psi_j(w_j) = x_0 + i. \tag{3.32}$$

Thus, in the single exponential case we have that

$$w_1 = \log(x_0 + i), \tag{3.33}$$

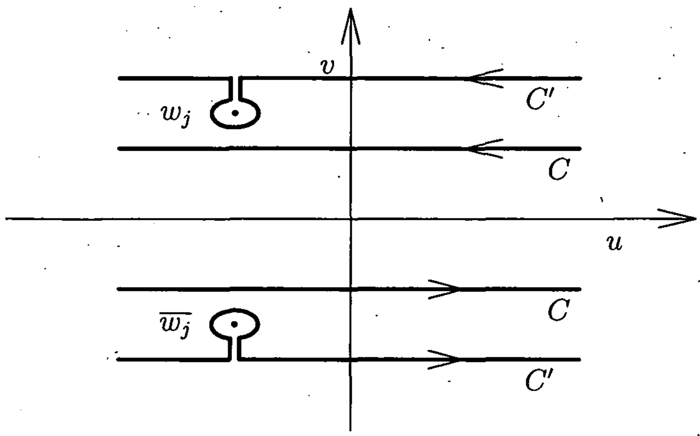

Figure 3.1: Contour integral representation of quadrature error - the contours C and C' in w-plane.

while in the double exponential case we have

$$w_2 = \operatorname{arcsinh}\left(\frac{2}{\pi}\log(x_0 + i)\right). \tag{3.34}$$

The residue of a function $g(w)$ at a simple pole w_0 is given by

$$\operatorname{Res}(g; w_0) = \lim_{w \to w_0} (w - w_0) g(w). \tag{3.35}$$

We deform the contour C around the poles w_j and $\overline{w_j}$ as depicted in Figure 3.1. As the radii of the arcs around w_j and $\overline{w_j}$ vanish the contribution to the integral from these arcs is given in terms of residues at these points. The contribution is negative due to the orientation of the contour. Furthermore, in the limit, the contributions from the vertical line segments exactly cancel.

Thus, in the limit, we obtain the representation

$$I - T_h^{(j)} = -\operatorname{Res}\Big(\frac{\Psi_h^T}{\Phi_h^T} f(\psi_j)\psi_j'; w_j\Big) - \operatorname{Res}\Big(\frac{\Psi_h^T}{\Phi_h^T} f(\psi_j)\psi_j'; \overline{w_j}\Big) + \frac{1}{2\pi i}\int_{C'} \frac{\Psi_h^T(w)}{\Phi_h^T(w)} f(\psi_j(w))\psi_j'(w)\, dw, \tag{3.36}$$

where C' is a positively described contour going above w_j and below $\overline{w_j}$ as depicted in Figure 3.1.

Neglecting the last integral and evaluating the residue terms we have that

$$\begin{aligned} I - T_h^{(j)} &\sim \frac{\pi \exp(i\frac{\pi}{h}w_j)}{\sin(\frac{\pi}{h}w_j)}\frac{1}{2i} + \frac{\pi \exp(-i\frac{\pi}{h}\overline{w_j})}{\sin(\frac{\pi}{h}\overline{w_j})}\frac{1}{2i} \\ &= \pi \left[\frac{1}{1-\exp(-2i\frac{\pi}{h}w_j)} + \frac{1}{1-\exp(2i\frac{\pi}{h}\overline{w_j})}\right], \end{aligned} \tag{3.37}$$

as $h \to 0$. We now substitute $w_j = u_j + iv_j$ and $\overline{w_j} = u_j - iv_j$ and rearrange to give

$$I - T_h^{(j)} \sim \pi \frac{\exp(-2\frac{\pi}{h}v_j) - \cos(2\frac{\pi}{h}u_j)}{\cosh(2\frac{\pi}{h}v_j) - \cos(2\frac{\pi}{h}u_j)}, \tag{3.38}$$

as $h \to 0$.

On neglecting the cosine term in the denominator, the exponential term in the numerator and replacing $\cosh(2\frac{\pi}{h}v_j)$ by $\exp(2\frac{\pi}{h}v_j)/2$ we obtain

$$I - T_h^{(j)} \sim -2\pi\cos(2\frac{\pi}{h}u_j)\exp(-2\frac{\pi}{h}v_j), \tag{3.39}$$

as $h \to 0$.

We shall now investigate the truncation error in the case that $x_0 = 0$. The truncation error $T_h^{(j)} - T_{n,h}^{(j)}$ is given by

$$T_h^{(j)} - T_{n,h}^{(j)} = h \sum_{|k|>n} f(\psi_j(kh))\psi_j'(kh). \tag{3.40}$$

In the single exponential case we have that

$$f(\psi_1(u))\psi_1'(u) = \frac{e^u}{e^{2u}+1}, \tag{3.41}$$

from which it evident that

$$f(\psi_1(u))\psi_1'(u) \sim \exp(-|u|), \tag{3.42}$$

as $u \to \pm\infty$. Hence, the truncation error behaves as

$$\begin{aligned} T_h^{(1)} - T_{n,h}^{(1)} &= h \sum_{|k|>n} f(\psi_1(kh))\psi_1'(kh) && (3.43) \\ &\sim h \sum_{|k|>n} e^{-|kh|} && (3.44) \\ &= 2h\frac{e^{-(n+1)h}}{1-e^{-h}} && (3.45) \\ &= \frac{2he^{-nh}}{e^h - 1}, && (3.46) \end{aligned}$$

as $h \to 0$. Now, making the approximation $e^h - 1 \sim h$, we have that

$$T_h^{(1)} - T_{n,h}^{(1)} = O(e^{-nh}), \tag{3.47}$$

while in the double exponential case, we have that

$$f(\psi_2(u))\psi_2'(u) = \frac{\pi}{4}\operatorname{sech}(\frac{\pi}{2}\sinh u)\cosh u. \tag{3.48}$$

As $u \to \pm\infty$, we have that $\sinh u \sim \pm e^{|u|}/2$, $\cosh u \sim e^{|u|}/2$, and $\operatorname{sech} u \sim 2e^{-|u|}$. These estimates combined with (3.48) imply that

$$f(\psi_2(u))\psi_2'(u) \sim \frac{\pi}{4}e^{-\frac{\pi}{4}e^{|u|}}e^{|u|}, \tag{3.49}$$

as $u \to \pm\infty$. Thus, in the double exponential case the truncation error is given by

$$T_h^{(2)} - T_{n,h}^{(2)} = h\sum_{|k|>n} f(\psi_1(kh))\psi_1'(kh) \tag{3.50}$$

$$\sim \frac{\pi h}{2}\sum_{k=n+1}^{\infty} e^{-\frac{\pi}{4}e^{kh}}e^{kh}, \tag{3.51}$$

as $h \to 0$. Now, take $e^h \sim 1$ and approximate this series by its first term to give

$$T_h^{(2)} - T_{n,h}^{(2)} = O\left(\exp\left(-\frac{\pi}{4}nh\exp(nh)\right)\right). \tag{3.52}$$

Thus, on equating exponents on the right of (3.39) and (3.47) we obtain

$$h^{(1)} = \sqrt{\frac{2\pi v_1}{n}}, \tag{3.53}$$

while from (3.39) and (3.52) we have that

$$8v_2 n = n^2h^2e^{nh}. \tag{3.54}$$

In order to explicitly determine $h^{(2)}$ in terms of n we rewrite equation (3.54) as

$$\log(8v_2n) = 2\log(nh) + nh. \tag{3.55}$$

If we now assume that $nh \to \infty$ as $n \to 0$ and $h \to \infty$, then the first term on the right is negligible and we obtain

$$h^{(2)} = \frac{1}{n}\log(8v_2n). \tag{3.56}$$

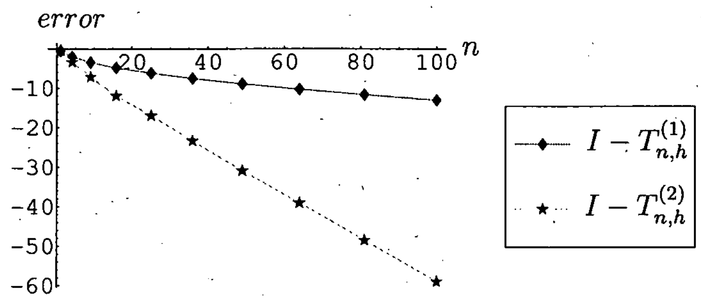

Figure 3.2: Single Exponential versus Double Exponential for the approximation of $\int_0^\infty (x^2+1)^{-1}\,dx$. We plot the base-10 logarithm of the error.

(It might be noted that Takahasi and Mori [23, eqn2.b.14] suggest, without justification, the choice $h^{(2)} = \frac{1}{n}\log(2\pi v_2 n)$.)

On substitution for h using (3.53) into (3.39) we obtain the following estimate of the overall error of the single exponential method

$$I - T_{n,h}^{(1)} \sim C\exp(-\sqrt{2\pi v_1 n}), \tag{3.57}$$

as $n \to \infty$. While, in the double exponential case, on substitution for h using (3.56) into (3.39) we obtain the following estimate of the overall error of the double exponential method

$$I - T_{n,h}^{(2)} \sim C\exp(-\frac{2\pi v_2 n}{\log(8v_2 n)}), \tag{3.58}$$

as $n \to \infty$.

From these estimates we see that the double exponential method is expected to perform asymptotically better than the single exponential method.

To illustrate this we approximate the integral I when $x_0 = 0$. In this case we have that

$$w_1 = \log(i) = i\frac{\pi}{2}, \tag{3.59}$$

$$w_2 = \log(\frac{2}{\pi}\operatorname{arcsinh}(i)) = \log(i) = i\frac{\pi}{2}, \tag{3.60}$$

that is, $v_1 = v_2 = \frac{\pi}{2}$.

Figure 3.2 shows the errors of the single exponential and the double exponential methods for $n = 1, 4, 9...100$. We see that the double exponential method achieves much higher accuracy than the single exponential method for a given number of function evaluations. In fact, when n is taken to be 100, the double exponential approximation is correct to approximately 60 decimal places while the single exponential approximation is correct to approximately 10 decimal places for the same number of function evaluations. (We have not included estimates of the errors in the graph. In all cases the estimates closely approximate the true errors.)

Chapter 4

Fourier Transforms and their Approximation

Fourier transforms and some existing methods for their numerical approximation are presented in this chapter. Our interest in the numerical approximation of Fourier transforms is motivated by the desire to evaluate the functions $S_0(a, b, t)$ and $C_1(a, b, t)$ defined in Chapter 2 (see (2.45) and (2.46)). The existing numerical methods presented in this chapter will be improved upon in the next chapter.

After defining the Fourier sine and cosine transforms in Section 4.1, we note some of their occurrences.

In Section 4.2 we define the Fourier cosine integral $C_0(a, b, t)$. We evaluate it in terms of trigonometric integrals Ci and Si. This integral is of interest as it occurs in Ooura and Mori [20] and [21] as examples on which they test their numerical method.

In Section 4.3 we look at some methods for the numerical approximation of Fourier transforms. We briefly review Filon's method [12] which is widely used. The method of Lund [15] uses the change of variable of Stenger $x = \sinh^{-1}(e^u)$, (see (3.24)) followed by the trapezoidal rule. In the case that the integrand has exponential decay this produces exponential convergence. In the case that the integrand decays only algebraically, it is necessary to speed the convergence of the trapezoidal sum by means of the Euler transform.

In Section 4.5 we focus on the methods of Ooura and Mori [20],[21]. These methods are again based on transforming the integral to one over the real line and then applying the trapezoidal rule. The properties of the particular change of variable used are of vital importance to these methods.

Ooura and Mori [20] introduce a change of variable to approximate the Fourier transforms of functions of algebraic decay without poles. In a later paper [21], they present a variation of this method which allows functions having poles. Furthermore, they note that their method produces slow convergence for the integral $C_0(2,1,1)$. Specifically, the rate of convergence of their method is limited due to the location of the poles.

4.1 Occurrence of Fourier Transforms

4.1.1 Fourier sine and cosine transforms

We follow the conventions of Erdélyi [11] in the definitions of the Fourier sine and cosine transforms. In Chapter 1 of [11] the Fourier cosine transform of f is defined as

$$\hat{f}_c(t) = \int_0^\infty f(x)\cos(tx)dx, \qquad 0 \le t < \infty, \tag{4.1}$$

while in Chapter 2 the Fourier sine transform of f is defined as

$$\hat{f}_s(t) = \int_0^\infty f(x)\sin(tx)dx, \qquad 0 < t < \infty. \tag{4.2}$$

4.1.2 Fourier transforms in applied mathematics

Fourier sine and cosine transforms are ubiquitous in applied mathematics and the standard reference of work Erdélyi [11] contains many particular cases. Yet no table will contain all transforms arising in practice. For example, the transforms S_0 and C_1 (see (2.45) and (2.46), respectively) arose from the fluid mechanics problem of Chapter 2, yet these do not appear in Erdélyi [11].

In this section we shall present a few examples of functions f and their Fourier transforms. We shall point out particular features of these functions, which must be taken into account in the numerical evaluation of their transforms.

Lund [15] and Ooura and Mori [20], [21] present many examples of Fourier transforms, some of which will be considered in the following sections.

An interesting recent occurrence of Fourier transforms requiring efficient and accurate approximation is in the book "The SIAM 100-Digit Challenge: A Study in High-accuracy Numerical Computing" by Bornemann et al. [3]. This book presents 10 artificial problems each requiring numerical evaluation to 10 significant figures. The authors of that book use the method of Ooura and Mori.

In Bornemann et al. [3, chap 1] the following integral is required to be evaluated to 10 significant figures

$$I = \int_0^1 x^{-1} \cos(x^{-1} \log x)\, dx. \tag{4.3}$$

First put $x = e^{-s}$, so that $dx = -e^{-s} ds$ and $dx/x = -ds$. Thus, the integral (4.3) is given by

$$I = \int_0^\infty \cos(se^s)\, ds. \tag{4.4}$$

On writing $se^s = u$ we have that $s = W(u)$ the Lambert W-function, thus we arrive at

$$I = \int_0^\infty W'(u) \cos u\, du. \tag{4.5}$$

For further details of the Lambert W- function see Corless et al. [7].

As a second example from Bornemann et al. [3, chap 9], the location (to 10 significant figures) of the maximum of the following function is to be found

$$I(\alpha) = (2 + \sin(10\alpha)) \int_0^2 x^\alpha \sin(\frac{\alpha}{2-x})\, dx, \tag{4.6}$$

for $0 \leq \alpha \leq 5$. Define $q(\alpha)$ to be the integral

$$q(\alpha) = \int_0^2 x^\alpha \sin(\frac{\alpha}{2-x})\, dx. \tag{4.7}$$

On setting $x = \frac{2t}{1+t}$, the integral $q(\alpha)$ can be expressed as

$$q(\alpha) = \int_0^\infty \left(\frac{2t}{1+t}\right)^\alpha \frac{1}{(1+t)^2} \sin(\frac{\alpha(1+t)}{2})\, dt. \tag{4.8}$$

In order to find the location of the maximum value of $I(\alpha)$, the authors' method requires numerical approximations of $q(\alpha)$ and $q'(\alpha)$.

These integrals are amenable to the methods developed by Ooura and Mori [20], [21], and also to those methods to be introduced in the next chapter.

4.2 Fourier transforms of rational functions

To encompass the integrals presented by Ooura and Mori [21] we define the function

$$C_0(a, b, t) = \int_0^\infty \frac{\cos(xt)}{(x-a)^2 + b^2}\, dx, \tag{4.9}$$

where $a \in \mathbb{R}$ and $b, t > 0$. Specifically, the integrals $C_0(0, 1, 1)$ and $C_0(2, 1, 1)$ were considered in [21].

We are able to evaluate the function $C_0(a, b, t)$ in terms of the trigonometric integrals Si and Ci defined below. We follow the standard reference work [1, §5.2] and define the trigonometric integrals as follows.

For $z \in \mathbb{C}$, we define the sine integral $\mathrm{Si}(z)$ as

$$\mathrm{Si}(z) = \int_0^z \frac{\sin t}{t} dt. \tag{4.10}$$

The sine integral Si is an entire function. A commonly used notation is $\mathrm{si}(z) = \frac{\pi}{2} - \mathrm{Si}(z)$.

For $z \in \mathbb{C}$ such that $|\arg z| < \pi$, we define the cosine integral $\mathrm{Ci}(z)$ as

$$\mathrm{Ci}(z) = \gamma + \log z + \int_0^z \frac{\cos t - 1}{t} dt, \tag{4.11}$$

where γ is Euler's constant, $\gamma \approx 0.577216$. The cosine integral Ci has a branch cut discontinuity along the negative real axis.

The functions Si and Ci occur as Fourier sine and cosine transforms. Specifically, for $|\arg a| < \pi$ and $y > 0$, we have that

$$\int_0^\infty \frac{\cos(xy)}{a+x}\,dx = -\operatorname{si}(ay)\sin(ay) - \operatorname{Ci}(ay)\cos(ay) \tag{4.12}$$

$$\int_0^\infty \frac{\sin(xy)}{a+x}\,dx = \operatorname{Ci}(ay)\sin(ay) - \operatorname{si}(ay)\cos(ay), \tag{4.13}$$

as in §1.1 (9) and §1.2 (10), respectively, of Erdélyi et al. [11].

Making a partial fraction expansion in (4.9) allows us to write $C_0(a,b,t)$ as

$$C_0(a,b,t) = \frac{1}{2ib}\int_0^\infty \frac{\cos(xt)}{x-a-ib}\,dx - \frac{1}{2ib}\int_0^\infty \frac{\cos(xt)}{x-a+ib}\,dx. \tag{4.14}$$

On using (4.12) we have the representation

$$\begin{aligned} C_0(a,b,t) &= \frac{1}{2ib}\left[-\operatorname{si}((-a-ib)t)\sin((-a-ib)t) - \operatorname{Ci}((-a-ib)t)\cos((-a-ib)t)\right] \\ &- \frac{1}{2ib}\left[-\operatorname{si}((-a+ib)t)\sin((-a+ib)t) - \operatorname{Ci}((-a+ib)t)\cos((-a+ib)t)\right]. \end{aligned} \tag{4.15}$$

This representation allows evaluation of $C_0(a,b,t)$ for arbitrary a, b, t in terms of the functions Si and Ci at complex arguments. High precision evaluation of these functions is provided by computer packages such as Mathematica. For a Fortran code for evaluating the sine and cosine integrals at complex arguments, see [2].

Note that it is possible to use a computer algebra package such as Mathematica or Maple to obtain the representation (4.15) from the definition (4.9) of C_0 as an integral. Care must be taken to ensure that the computer algebra package treats special functions in the complex plane correctly.

4.3 Miscellaneous Quadrature Methods

The numerical evaluation of Fourier integrals is difficult due both to the infinite range of integration and the oscillatory integrand. Furthermore, possible hindrances include singularities of the function f on or near the interval of integration and its slow decay rate towards ∞. These difficulties are displayed in the following Fourier integrals.

The integrand in

$$\int_0^\infty \frac{\sin x}{\sqrt{x}}\,dx, \tag{4.16}$$

has a branch point singularity at $x = 0$. The integrand in

$$\int_0^\infty \frac{\cos x}{(x-2)^2+1}\,dx, \tag{4.17}$$

has a pair of poles $x = 2 \pm i$.

The integrand in

$$\int_0^\infty \frac{\sin x}{x+1}\,dx \tag{4.18}$$

decays algebraically at $+\infty$, while

$$\int_0^\infty \operatorname{sech} x \sin x\,dx. \tag{4.19}$$

has an exponentially decaying integrand.

4.3.1 Filon's Method

Filon's method is a popular method to evaluate numerically Fourier transforms. For $\hat{f}_s(t)$ it involves considering intervals between successive zeros of $\sin(tx)$ and fitting a cubic (or quadratic) polynomial to $f(x)\sin(tx)$ at equally spaced point choosing the zeros as the endpoints. A convergence acceleration method, such as the Euler transformation(see Section 4.3.2), can also be employed. For further details of this method see Abramowitz and Stegun [1, pp. 890-891] or the original paper by Filon [12].

4.3.2 Lund's Method

Lund [15] presents a method for the approximation of Fourier sine and cosine transforms.

The method proceeds in the same way for approximating either $\hat{f}_s(t)$ or $\hat{f}_c(t)$. We shall deal with $\hat{f}_s(t)$ as defined in (4.2).

Lund makes the change of variable $x = \sinh^{-1}(e^u) = \log(e^u + \sqrt{e^{2u}+1})$ to give the representation

$$\hat{f}_s(t) = \int_{-\infty}^{\infty} f(\sinh^{-1}(e^u)) \sin(t \sinh^{-1}(e^u)) \frac{e^u}{\sqrt{e^{2u}+1}}\, du. \tag{4.20}$$

The trapezoidal rule with stepsize $h > 0$ is then applied to this representation. This infinite trapezoidal sum can be truncated at $\pm n$ for a particular positive integer n. This transformation was used by Stenger [22] for the quadrature of exponentially decaying integrands as was discussed in Section 3.3.1.

The above method works well for functions that satisfy the following two conditions. Firstly, it is required that $f(x)$ decay exponentially towards $+\infty$ and has, at worst, an integrable singularity at 0, that is,

$$|f(x)| \leq C_1 x^{\alpha-1}, \quad 0 < x < 1,$$
$$|f(x)| \leq C_2 e^{-\alpha x}, \qquad x \geq 1,$$

where C_1, C_2 and α are positive constants. Secondly, it is required that the transformed integrand be analytic inside a strip of width $d < \frac{\pi}{2}$. Under these two conditions the choice

$$h = \sqrt{\frac{2\pi d}{\alpha n}} \tag{4.21}$$

results in convergence of order $O(\exp(-\sqrt{2\pi d\alpha n}))$ as $n \to \infty$. For further details and examples see Section 2 of Lund [15]

In the absence of exponential decay towards $+\infty$, the above procedure is hindered by the exceedingly large number of terms of the trapezoidal sum that must be taken to match the discretisation error. In this case Lund proposes that the convergence of the trapezoidal sum may be accelerated by the use of the Euler transformation [1, 3.6.27]. The Euler transformation of the alternating series

$$s = \sum_{k=0}^{\infty} (-1)^k a_k \tag{4.22}$$

is defined to be

$$s = \sum_{k=0}^{\infty} \frac{(-1)^k \Delta^k a_0}{2^{k+1}}, \tag{4.23}$$

where Δ^k, the k-th forward difference, is defined by

$$\Delta^k a_0 = \sum_{m=0}^{k} (-1)^m \begin{pmatrix} k \\ m \end{pmatrix} a_{k-m}. \tag{4.24}$$

For further details and examples, see Section 3 of [15].

4.4 Exponentially Convergent Quadrature Methods For Fourier Transforms

In this section we present a method for the approximation of Fourier integrals which is highly accurate and applicable to a wide range of functions, including those with singularities and algebraic decay. This method was first introduced by Ooura and Mori [20].

The method of approximation to $\hat{f}_s(t)$ is obtained by making a particular change of variable to pass from the interval $(0, \infty)$ to the interval $(-\infty, \infty)$, followed by an application of the trapezoidal rule. For $\hat{f}_c(t)$ we apply the same change of variable, but then we use the midpoint rule instead of the trapezoidal rule. The details of the change of variable are crucial in determining the characteristics of the method. The outlying quadrature points are chosen to coincide approximately with the zeros of the integrand. This allows the infinite trapezoidal sum to be truncated without introducing too large an error.

We describe the method for a general transformation $\phi(u)$. In the next section we shall describe the particular transformations $\phi_1(u)$ and $\phi_2(u)$ used by Ooura and Mori [20], [21]. Starting from their work we shall introduce two single exponential transformations $\phi_3(u)$ and $\phi_4(u)$ in the next chapter.

In order to approximate $\hat{f}_s(t)$ we take the definition (4.2) and make the change of variable

$$x = m\phi(u)/t, \qquad -\infty < u < \infty, \tag{4.25}$$

where $m > 0$ and $\phi : (-\infty, \infty) \rightarrow (0, \infty)$ is an increasing function satisfying

$$\phi(u) \rightarrow 0, \qquad \text{as} \qquad u \rightarrow -\infty, \tag{4.26}$$

$$\phi(u) \rightarrow u, \qquad \text{as} \qquad u \rightarrow +\infty. \tag{4.27}$$

Thus, $\hat{f}_s(t)$ can be represented by the integral

$$\hat{f}_s(t) = \int_{-\infty}^{\infty} F_m(u)\, du \tag{4.28}$$

where the function $F_m(u)$ is defined by

$$F_m(u) = f(m\phi(u)/t)\sin(m\phi(u))m\phi'(u)/t. \tag{4.29}$$

We now apply the trapezoidal rule (see equation (3.2)) with stepsize h to (4.28) to give the approximation

$$T_h = h \sum_{k=-\infty}^{\infty} F_m(kh). \tag{4.30}$$

Choosing

$$hm = \pi \tag{4.31}$$

together with the asymptotic behaviour of $\phi(u)$ at $\pm\infty$ given by (4.26) and (4.27) allows the infinite trapezoidal sum to be truncated without introducing too large an error. Further details will be presented in Section 5.4.

To approximate $\hat{f}_c(t)$ we apply the same change of variable, but then we apply the midpoint rule (3.8) to the transformed integral. Thus, we approximate $\hat{f}_c(t)$ by

$$M_h = h \sum_{k=-\infty}^{\infty} F_m((k+1/2)h), \tag{4.32}$$

where $m > 0$ and $F_m(u)$ is now defined by

$$F_m(u) = f(m\phi(u)/t)\cos(m\phi(u))m\phi'(u)/t. \tag{4.33}$$

4.5 Ooura and Mori's two double exponential transformations

Ooura and Mori introduced the transformation $\phi_1(u)$ (see (4.36)) in [20], and subsequently provided an analysis of this method in [21]. In the last paper they also introduced the transform $\phi_2(u)$ (see (4.41)) in order to solve problems arising from their first method. In their papers Ooura and Mori do not provide details of how they obtain their estimates of the discretisation error. Consequently, in this section we can only present their estimates without showing the necessary steps to derive them.

Ooura and Mori's transforms are double exponential, that is, they are asymptotic to 0 at $-\infty$ and u at $+\infty$ and approach these limits at double exponential rate. Specifically, for some $\alpha > 0$ they have the following properties:

$$\phi(u) \sim \exp(-\alpha \exp(-u)), \tag{4.34}$$

as $u \longrightarrow -\infty$ and

$$\phi(u) \sim u + \exp(-\alpha \exp(u)), \tag{4.35}$$

as $u \longrightarrow +\infty$.

Ooura and Mori [20, eqn (11)] introduce the first double exponential transformation $\phi_1(u)$ defined by

$$\phi_1(u) = \frac{u}{1 - \exp(-K \sinh u)}, \tag{4.36}$$

for $K > 0$. They make the choice of $K = 2\pi$ which produces good results for Fourier transforms with entire integrands such as

$$I_1 = \int_0^\infty \frac{\sin x}{x}\, dx. \tag{4.37}$$

They quote [21, eqn (2.9)] the discretisation error,

$$|I_1 - T_h| = O(\exp(-\frac{2.32}{h})) = O(\exp(-\frac{2.32m}{\pi})), \tag{4.38}$$

as $h \to 0$ or, equivalently $m \to \infty$.

However, for integrands with poles the method does not perform as well. In fact, they consider the integral

$$I_2 = \int_0^\infty \frac{\cos x}{x^2 + 1}\, dx, \tag{4.39}$$

with poles at $\pm i$. This integral is an instance of the function $C_0(a, b, t)$ as defined in (4.9), in particular, $I_2 = C_0(0, 1, 1)$. In this case they claim [21, eqn (2.12)] that the error behaves as

$$|I_2 - M_h| = O(\exp(-\frac{\pi^2 - \delta}{h \log(\pi/h)})) = O(\exp(-\frac{\pi^2 - \delta}{\frac{\pi}{m} \log(m)})), \tag{4.40}$$

as $h \to 0$, or equivalently $m \to \infty$ and where δ is a small positive number. This rate of convergence is slow relative to the rate (4.38) for integrands without poles.

In order to rectify this, Ooura and Mori [21, eqn (3.3)] introduce the second double exponential transformation $\phi_2(u)$ defined to be

$$\phi_2(u) = \frac{u}{1 - \exp(-2u - \alpha(1 - e^{-u}) - \beta(e^u - 1))} \tag{4.41}$$

where the parameters α and β are given by [21, eqn (3.6)]

$$\alpha = \beta / \sqrt{1 + m \log(1 + m)/(4\pi)}, \quad \beta = \frac{1}{4}. \tag{4.42}$$

Note that the parameter α is given in terms of the parameter m introduced in equation (4.25).

Using this transformation the authors claim that the discretisation error behaves like

$$|I_2 - M_h| = O(\exp(-\frac{4.75}{h})) = O(\exp(-\frac{4.75m}{\pi})), \tag{4.43}$$

as $h \to 0$, or equivalently $m \to \infty$, see [21, eqn (3.14)].

Finally, in their second paper they give the integral (see [21, eqn (4.15)])

$$I_3 = \int_0^\infty \frac{\cos x}{(x-2)^2 + 1} \, dx, \tag{4.44}$$

as an example of an integral for which neither of their methods performs well. This integrand has poles at $2 \pm i$.

This integral is an instance of the function $C_0(a, b, t)$ as defined in (4.9), specifically, we see that $I_3 = C_0(2, 1, 1)$.

We shall return to this example in Section 5.6, where we propose a simple relation that allows the approximation of I_3 with a high rate of exponential convergence.

Chapter 5

Single Exponential Approximation of Fourier Transforms

In this chapter we present a new method for the approximate evaluation of Fourier transforms. We will present a single exponential version of the two double exponential transformations of Ooura and Mori presented in the previous chapter. This chapter is the core of this thesis and contains the bulk of the new results.

We are primarily concerned with Fourier transforms of rational functions. The physical problem of Chapter 2 resulted in a solution u which was a linear combination of Fourier transforms of rational functions (see equation (2.47)). Furthermore, the following two integrals were presented by Ooura and Mori [20, 21] and discussed in the previous chapter

$$C_0(0,1,1) = \int_0^\infty \frac{\cos x}{x^2+1}\,dx \qquad C_0(2,1,1) = \int_0^\infty \frac{\cos x}{(x-2)^2+1}\,dx. \tag{5.1}$$

They are particular instances of the function $C_0(a,b,t)$ as defined in equation (4.9).

The approximate evaluation of $C_0(0,1,1)$ was handled by Ooura and Mori [21] by introducing the transformation $\phi_2(u)$, defined by equations (4.41) and (4.42). This transformation seems complicated and the arising analysis is messy. Furthermore, the approximate evaluation of $C_0(2,1,1)$ was posed by them as an open problem.

In Section 5.1 we introduce a method of the type described in Section 4.4 for the approximation of Fourier integrals . This method is based on a new transformation $\phi_3(u)$, defined in equation (5.2). This transformation is much simpler than the transformation $\phi_2(u)$ of Ooura and Mori. Our new method achieves exponential convergence for Fourier integrals of functions with poles, including $C_0(0,1,1)$ and $C_0(2,1,1)$ given above.

In Section 5.3 we analyse the discretisation error of our method when applied to the integral $C_0(a,b,t)$. We shall see that it depends on the proximity of the poles of the integrand to the positive real axis. We see that, while our method produces exponential convergence for the approximation of $C_0(2,1,1)$, the convergence is slow when compared with the rate for $C_0(0,1,1)$.

We then analyse the truncation error with the aim of matching the discretisation error so that we can relate n and h. Also, in Section 5.4, we determine the overall convergence rate of our method.

Finally, we compare our method with the method developed by Ooura and Mori using the transformation $\phi_2(u)$. In terms of the number of function evaluations our method produces asymptotically slower convergence than the method of Ooura and Mori. However, for moderate n our single exponential method competes with their double exponential method.

However, it should be noted that the number of function evaluations required may not be the best measure of comparison for the two methods as each requires the computation of quadrature weights and points. From the complicated nature of their transform (see equation (4.41)) compared to ours (see equation (5.2)) we see that the computation of quadrature weights and point required by their method has a much higher cost than the cost of computation of quadrature weights and points required by our method.

Furthermore, the simplicity of our transformation allows for an extensive analysis of the associated discretisation error as detailed in Section 5.3. In comparison, the results of their analysis, presented in Section 4.5, are cumbersome. Furthermore, they have not published details of how they have derived these results.

In Section 5.7 we propose a simple remedy to allow our method to achieve a higher rate of convergence. In doing this we provide a solution to the open problem posed by Ooura and Mori.

At the end of this chapter we present our second single exponential transform $\phi_4(u)$ and briefly compare it to our first transform ϕ_3.

5.1 Single Exponential Transformation I

The basis of our method is provided by the following single exponential transformation which has the required properties (4.26) and (4.27) but is of a simpler form than Ooura and Mori's double exponential transformations.

We define the transformation $\phi_3 : (-\infty, \infty) \to (0, \infty)$ by

$$\phi_3(u) = \log(e^u + 1), \qquad -\infty < u < \infty. \tag{5.2}$$

The derivative $\phi_3'(u)$ is given by

$$\phi_3'(u) = \frac{e^u}{e^u + 1}. \tag{5.3}$$

For the analysis of the truncation error we shall need to know the asymptotic behaviour of $\phi_3(u)$ as $u \to \pm\infty$. The Taylor series of $\log(1 + x)$ around $x = 0$ is given by

$$\log(1 + x) = x + O(x^2), \text{ as } x \to 0, \tag{5.4}$$

see [1, eqn 4.1.24]. Thus, we have that

$$\phi_3(u) = e^u + O(e^{2u}), \tag{5.5}$$

as $u \to -\infty$, and

$$\phi_3(u) = u + \log(1 + e^{-u}) = u + e^{-u} + O(e^{-2u}), \tag{5.6}$$

as $u \to \infty$. Furthermore, we have that

$$\phi_3'(u) = e^u(1 + e^u)^{-1} = e^u + O(e^{2u}), \tag{5.7}$$

as $u \to -\infty$, and

$$\phi_3'(u) = (1 + e^{-u})^{-1} = 1 + O(e^{-u}), \tag{5.8}$$

as $u \to \infty$.

Note that as a function of the complex variable $w = u + iv$, $\phi_3(w)$ has branch points at $w = (2k+1)i\pi$ for any integer k. The inverse $\phi_3^{-1} : (0, \infty) \to (-\infty, \infty)$ is given by

$$\phi_3^{-1}(x) = \log(e^x - 1), \qquad 0 < x < \infty. \tag{5.9}$$

For the analysis of the discretisation error we shall determine the asymptotic behaviour of $w = \phi_3^{-1}(z)$ as $z \to 0$ when $\phi_3^{-1}(x)$, as given by (5.9), is extended to the complex z-plane. From (5.9) we have

$$w = \log(e^z - 1) = \log z + \log \frac{e^z - 1}{z}. \tag{5.10}$$

On expanding the last term about $z = 0$, we arrive at

$$w = \log z + \frac{z}{2} + O(z^2), \tag{5.11}$$

as $z \to 0$.

In the case that z is purely imaginary we are able to obtain a neat representation of $\phi_3^{-1}(z)$. In fact, if $z = iy$ for $0 < y < \pi$ we have from (5.9) that

$$\begin{aligned}
\phi_3^{-1}(iy) &= \log(e^{iy} - 1) \\
&= \log \sqrt{(\cos y - 1)^2 + (\sin y)^2} + i \arctan\left(\frac{\sin y}{\cos y - 1}\right) \\
&= \log(2 \sin \frac{y}{2}) + i(y + \pi)/2.
\end{aligned} \tag{5.12}$$

We restrict ourselves to the case $0 < y < \pi$ as this is all that is neeeded for the analysis of the discretisation error to follow in Section 5.3.1.

5.2 Application of our method to the Cosine Integral

In this section we apply our method to the integral $C_0(a, b, t)$ as defined in equation (4.9) for $a \in \mathbb{R}$ and $b, t > 0$. We note that the integrand has simple poles at $a \pm ib$. The integrals considered by Ooura and Mori were of this form. In fact, $C_0(0, 1, 1)$ was of prime importance in [21], while the approximation of $C_0(2,1,1)$ was left as an open problem. For ease of notation we denote $C_0(a,b,t)$ by I where the values of a,b,t are clear from the context.

We estimate the discretisation error using residues and the saddle point method. We shall see that the discretisation error depends on the proximity of the singularities of the integrand $a \pm ib$ to the interval of integration $(0,\infty)$.

In order to implement our method we first make the change of variable $x = m\phi_3(u)/t$ and apply the midpoint rule with stepsize h to arrive at the approximation

$$M_h = h \sum_{k=-\infty}^{\infty} F_m((k+1/2)h), \tag{5.13}$$

where the function $F_m(u)$ is given by

$$F_m(u) = \frac{\cos(m\phi_3(u))m\phi_3'(u)/t}{(m\phi_3(u)/t-a)^2+b^2} = mt\frac{\cos(m\phi_3(u))\phi_3'(u)}{(m\phi_3(u)-at)^2+b^2t^2}. \tag{5.14}$$

As usual we choose h and m such that $mh = \pi$.

5.3 Discretisation error

We shall denote the pole of $F_m(w)$ in the upper-half plane closest to the real axis by w_0. Specifically, from (5.14), it is evident that w_0 is given as the solution to the equation

$$\phi_3(w_0) = (a+ib)t/m, \tag{5.15}$$

that is in the upper half plane and is closest to the real axis. Note that $\overline{w_0}$ is also a pole of $F_m(w)$.

Now, from equation (3.9) we have that

$$I - M_h = \frac{1}{2\pi i}\int_C \frac{\Psi_h^M(w)}{\Phi_h^M(w)} F_m(w)\,dw, \tag{5.16}$$

where $\Psi_h^M(w)$ and $\Phi_h^M(w)$ are given by (3.10) and (3.11) respectively, and where C is a positively described contour, passing between the real axis and the poles w_0 and $\overline{w_0}$ as depicted in Figure 5.1. Furthermore, we assume that the contour C avoids the branch points of ϕ_3 which lie at $(2k+1)i\pi, k \in \mathbb{Z}$.

We deform the contour C around the poles w_0 and $\overline{w_0}$ as depicted in Figure 5.1. As the radii of the arcs around w_0 and $\overline{w_0}$ vanish the contribution to the integral from these arcs is given in terms of residues at these points. The contribution is negative due to the orientation of the contour. Furthermore, in the limit, the contributions from the vertical line segments exactly cancel.

Thus, in the limit, we obtain the representation

$$I - M_h = -\operatorname{Res}(\frac{\Psi_h^M}{\Phi_h^M}F_m; w_0) - \operatorname{Res}(\frac{\Psi_h^M}{\Phi_h^M}F_m; \overline{w_0}) + \frac{1}{2\pi i}\int_{C'} \frac{\Psi_h^M(w)}{\Phi_h^M(w)}F_m(w)\, dw, \qquad (5.17)$$

where C' is a positively described contour going above w_0 and below $\overline{w_0}$ as depicted in Figure 5.1. Again, we assume that the contour C' avoids the branch points of ϕ_3 which lie at $(2k+1)i\pi, k \in \mathbb{Z}$.

In equation (5.17) we shall denote sum of the two residue terms by R_h and the integral over C' term by S_h. Thus, we have

$$R_h = -\operatorname{Res}(\frac{\Psi_h^M}{\Phi_h^M}F_m; w_0) - \operatorname{Res}(\frac{\Psi_h^M}{\Phi_h^M}F_m; \overline{w_0}) \qquad (5.18)$$

and

$$S_h = \frac{1}{2\pi i}\int_{C'} \frac{\Psi_h^M(w)}{\Phi_h^M(w)}F_m(w)\, dw, \qquad (5.19)$$

so that

$$I - M_h = R_h + S_h. \qquad (5.20)$$

5.3.1 Contribution to the error from the poles

In this section, to determine contribution of the poles to the discretisation error, we evaluate the residue terms R_h as defined in equation (5.18).

Using L'Hopital's rule, the residue of $F_m(w)$ (as defined in equation (5.14)) at w_0 is given by

$$\begin{aligned} \operatorname{Res}(F_m; w_0) &= \lim_{w\to w_0}(w-w_0)mt\frac{\cos(m\phi_3(w))\phi_3'(w)}{(m\phi_3(w)-at)^2+b^2t^2} \\ &= t\frac{\cos(m\phi_3(w_0))}{2(m\phi_3(w_0)-at)}. \end{aligned} \qquad (5.21)$$

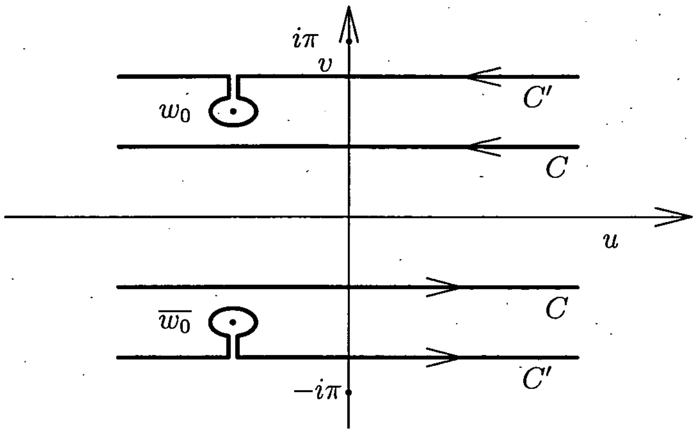

Figure 5.1: Contour integral representation of quadrature error - the contours C and C' in w-plane.

Now, from equation (5.15) we have that

$$\operatorname{Res}(F_m; w_0) = \frac{\cos((a+ib)t)}{2ib}. \tag{5.22}$$

Similarly, we have that the residue of $F_m(w)$ at $\overline{w_0}$ is given by

$$\operatorname{Res}(F_m; \overline{w_0}) = -\frac{\cos((a-ib)t)}{2ib}. \tag{5.23}$$

Combining these residues with the definitions of $\Psi_h^M(w)$ and $\Phi_h^M(w)$ (see (3.10) and (3.11) respectively), we have that

$$\begin{aligned} R_h &= \frac{\pi \exp(imw_0)}{\cos(mw_0)} \frac{\cos(a+ib)t}{2b} + \frac{\pi \exp(-im\overline{w_0})}{\cos(m\overline{w_0})} \frac{\cos(a-ib)t}{2b} \\ &= \frac{\pi}{b}\left[\frac{\cos(a+ib)t}{1+\exp(-2imw_0)} + \frac{\cos(a-ib)t}{1+\exp(2im\overline{w_0})}\right]. \end{aligned} \tag{5.24}$$

We now substitute $w_0 = u_0 + iv_0$ and $\overline{w_0} = u_0 - iv_0$ and rearrange to give

$$R_h = \frac{\pi}{b} \frac{\cos(at)\cosh(bt)(\exp(-2mv_0) + \cos(2mu_0)) + \sin(at)\sinh(bt)\sin(2mu_0)}{\cosh(2mv_0) + \cos(2mu_0)}. \tag{5.25}$$

Neglecting the cosine term in the denominator and the exponential term $\exp(-2mv_0)$ in the numerator we have that

$$R_h \sim \frac{2\pi}{b} \frac{\cos(at)\cosh(bt)\cos(2mu_0) + \sin(at)\sinh(bt)\sin(2mu_0)}{\exp(2mv_0) + \exp(-2mv_0)}, \tag{5.26}$$

as $h \to 0$ or equivalently $m \to \infty$. On neglecting the term $\exp(-2mv_0)$ in the denominator, we obtain

$$R_h \sim \frac{2\pi}{b}(\cos(at)\cosh(bt)\cos(2mu_0) + \sin(at)\sinh(bt)\sin(2mu_0))\exp(-2mv_0), \quad (5.27)$$

as $h \to 0$ or equivalently $m \to \infty$. (Note that in the case of small b it is not justified to neglect the cosine and exponential terms in equation (5.25). In this thesis we do not analyse the case of small b. In fact, we only consider the case $b = 1$.)

In the case $a = 0$ we have from (5.12) that

$$v_0 = \frac{\pi}{2} + \frac{bt}{2m} \quad (5.28)$$

While in the case $a \neq 0$ we are content in knowing the asymptotic behaviour of w_0 as $m \to \infty$, which we can obtain from (5.11):

$$w_0 = \log\frac{(a+ib)t}{m} + \frac{(a+ib)t}{2m} + O(m^{-2}), \quad (5.29)$$

as $m \to \infty$.

For $a > 0$ we have that

$$\Im\left(\log\frac{(a+ib)t}{m}\right) = \arctan(\frac{b}{a}), \quad (5.30)$$

while for $a < 0$ we have that

$$\Im\left(\log\frac{(a+ib)t}{m}\right) = \pi + \arctan(\frac{b}{a}). \quad (5.31)$$

Thus, it follows that the imaginary part v_0 of w_0 has asymptotic behaviour

$$v_0 = \begin{cases} \arctan(\frac{b}{a}) + \frac{bt}{2m} + O(\frac{1}{m^2}), & a > 0, \\ \frac{\pi}{2} + \frac{bt}{2m}, & a = 0 \\ \pi + \arctan(\frac{b}{a}) + \frac{bt}{2m} + O(\frac{1}{m^2}), & a < 0. \end{cases} \quad (5.32)$$

as $m \to \infty$. Furthermore, in the next section we provide an alternative derivation in the case that $a \neq 0$.

Thus, using the asymptotic estimates (5.27) and (5.32), we have the estimate

$$R_h \sim \begin{cases} C\exp\left(-2m\arctan(\frac{b}{a})\right), & a>0, \\ C\exp\left(-m\pi\right)), & a=0 \\ C\exp\left(-2m(\pi+\arctan(\frac{b}{a}))\right), & a<0, \end{cases} \tag{5.33}$$

as $m \to \infty$, where C represents a number independent of m.

5.3.2 Alternative derivation of asymptotic behaviour of image of pole

Here we present an alternative derivation of the asymptotic behaviour of v_0 as $m \to \infty$ to that provided in equation (5.32). This result was used in the previous section to estimate the contribution R_h to the error $I - M_h$. We only consider the case $a > 0$ and we shall investigate $h = \pi/m \to 0$ instead of $m \to \infty$.

From equation (5.9) and (5.15) the point w_0 is given by

$$\begin{aligned} w_0 &= \log(e^{(a+ib)th/\pi} - 1) \\ &= \log(e^{ath/\pi}\cos(bth/\pi) - 1 + ie^{ath/\pi}\sin(bth/\pi)). \end{aligned} \tag{5.34}$$

As before we denote the real and imaginary parts of w_0 by u_0 and v_0, respectively. If we explicitly denote the dependence of v_0 on h by $v_0(h)$ we have that

$$v_0(h) = \arctan\left(\frac{\sin(bth/\pi)}{\cos(bth/\pi) - e^{-ath/\pi}}\right). \tag{5.35}$$

As $h \to 0$, we have that

$$\begin{aligned} \lim_{h\to 0} v_0(h) &= \arctan\left(\lim_{h\to 0}\frac{\sin(bth/\pi)}{\cos(bth/\pi) - e^{-ath/\pi}}\right) \\ &= \arctan\left(\lim_{h\to 0}\frac{bt\cos(bth/\pi)/\pi}{-bt\sin(bth/\pi)/\pi + ate^{-ath/\pi}/\pi}\right) \\ &= \arctan(\frac{b}{a}). \end{aligned} \tag{5.36}$$

After a lengthy calculation, we find

$$\lim_{h\to 0}\frac{v_0(h) - v_0(0)}{h} = \frac{bt}{2\pi}. \tag{5.37}$$

On, combining (5.36) and (5.37) we have that

$$v_0(h) = \arctan(\frac{b}{a}) + \frac{bt}{2\pi}h + O(h^2), \tag{5.38}$$

as $h \to 0$. In terms of m this results in

$$v_0 = \arctan(\frac{b}{a}) + \frac{bt}{2m} + O(m^{-2}), \tag{5.39}$$

as $m \to \infty$. This agrees with the result presented in equation (5.32).

We include this technique as it can be used in connection with other quadrature rules, for example, Ooura and Mori's transformations ϕ_1 and ϕ_2 or our second single exponential transformation ϕ_4 which features in the last section of this chapter.

5.3.3 Saddle Point Approximation according to de Bruijn

Given a contour integral $I_m = \int_\Gamma F(w)\,dw$ dependent on a large positive parameter m we present the saddle point approximation following Chapter 5 of de Bruijn [9].

Firstly, the integrand $F(w)$ is factorised as $\exp(mp(w))q_m(w)$ for some functions $p(w)$ and $q_m(w)$ such that $p(w)$ is independent of m. Let w_1 denote a saddle point of $p(w)$, that is, a point at which $p'(w_1) = 0$ and $p''(w_1) \neq 0$. Deform Γ into the curve Γ_1 such that (i) Γ_1 passes through w_1 and (ii) $\Re p(w)$ decreases most rapidly along Γ_1. This curve is known as the curve of steepest descent. Thus we have the representation

$$I_m = \int_{\Gamma_1} \exp(mp(w))q_m(w)\,dw. \tag{5.40}$$

Now, approximate I_m by (i) approximating $p(w)$ by its second order Taylor approximation at w_1, (ii) approximating $q_m(w)$ by $q_m(w_1)$ and (iii) replacing Γ_1 by its tangent at w_1. Having made these approximations we arrive at equation (5.7.2) of De Bruijn [9]:

$$I_m \sim \sqrt{\frac{2\pi}{m|p''(w_1)|}}\alpha e^{mp(w_1)} q_m(w_1), \tag{5.41}$$

as $m \to \infty$, where $|\alpha| = 1$ and

$$\arg\alpha = \frac{\pi}{2} - \frac{1}{2}\arg(p''(w_1)), \tag{5.42}$$

is the angle at which Γ_1 passes through w_1. The choice of p and q is somewhat arbitrary, but it is intended that w_1 is easily determined and that $q_m(w)$ does not vary greatly in a neighbourhood of w_1.

5.3.4 Contribution to the error from the saddle points

In this section we estimate the contribution to the error $I - M_h$ from the integral S_h as defined in (5.19) using the saddle point method as described in the previous section.

Recall that S_h is defined as an integral over the contour C' as depicted in Figure 5.1. We denote the upper half of C' by C'_+ and the lower half of C' by C'_-. Assuming that the contributions to S_h from C'_+ and C'_- are conjugates we have that

$$S_h = 2\Re\left(\frac{1}{2\pi i}\int_{C'_+}\frac{\Psi_h^M(w)}{\Phi_h^M(w)}F_m(w)\,dw\right). \tag{5.43}$$

On using (3.10), (3.11), (5.2) and (5.14), we have that

$$S_h = -mt\Re\left(\int_{C'_+}\frac{e^{imw}}{\cos(mw)}\frac{\cos(m\log(e^w+1))}{(m\log(e^w+1)-at)^2+b^2t^2}\frac{e^w}{e^w+1}\,dw\right). \tag{5.44}$$

We make the choice

$$p(w) = i(2w - \log(e^w+1)), \tag{5.45}$$

in which case it follows that

$$q_m(w) = \frac{e^{2im\log(e^w+1)}+1}{e^{2imw}+1}\frac{1}{(m\log(e^w+1)-at)^2+b^2t^2}\frac{e^w}{e^w+1}. \tag{5.46}$$

The saddle points of $p(w)$ are solutions of the equation $p'(w) = 0$. On differentiation we have

$$p'(w) = i(2 - \frac{e^w}{e^w+1}). \tag{5.47}$$

The saddle points of $p(w)$ are given as solutions to the equation

$$e^w = -2. \tag{5.48}$$

or

$$w_k = \log 2 + (2k-1)\pi i, \tag{5.49}$$

where $k \in \mathbb{Z}$. Let the saddle point in the upper half plane closest to the real axis be denoted by w_1 thus, we have that

$$w_1 = \log 2 + i\pi. \tag{5.50}$$

We now deform the contour C'_+ into $C'_{+,1}$, the curve of steepest descent through w_1. Thus, we have the representation

$$S_h = -mt\Re\left(\int_{C'_{+,1}} e^{mp(w)} q_m(w)\, dw\right). \tag{5.51}$$

Now, applying the saddle point approximation (5.41) to the integral in (5.51) we arrive at

$$S_h \sim -mt\Re\left(\sqrt{\frac{2\pi}{m|p''(w_1)|}}\alpha e^{mp(w_1)} q_m(w_1)\right), \tag{5.52}$$

as $m \to \infty$.

We shall need the fact that

$$p''(w_1) = -i\frac{e^{w_1}}{e^{w_1}+1} = 2i, \tag{5.53}$$

from which it follows that

$$|p''(w_1)| = 2, \tag{5.54}$$

and

$$\arg p''(w_1) = (2k + 1/2)\pi, \tag{5.55}$$

for any integer k. From (5.42), we have that the angle at which C'_{+1} passes through w_1 is given by

$$\arg(\alpha) = \frac{\pi}{2} - \frac{1}{2}\arg(p''(w_1)) = (-k + \frac{1}{4})\pi. \tag{5.56}$$

Because the original contour C was positively described, we take $k = 1$ to give

$$\arg \alpha = -\frac{3\pi}{4}, \tag{5.57}$$

so that

$$\alpha = e^{-i\frac{3\pi}{4}}. \tag{5.58}$$

From (5.45) and (5.50) we have that

$$p(w_1) = -\pi + i \log 4 \tag{5.59}$$

and from (5.46) and (5.50) we have that

$$q_m(w_1) = \frac{e^{-2m\pi} + 1}{e^{-2m\pi} e^{im \log 4} + 1} \frac{2}{(a^2 + b^2)t^2 - m^2\pi^2 - 2\pi imat}. \tag{5.60}$$

On substitution of (5.54), (5.58), (5.59) and (5.60) into (5.52) we have that

$$S_h \sim -mt\Re \left(\sqrt{\frac{\pi}{m}} e^{-\frac{3\pi}{4}i} e^{m(-\pi + i \log 4)} \frac{e^{-2m\pi} + 1}{e^{-2m\pi} e^{im \log 4} + 1} \frac{2}{(a^2 + b^2)t^2 - m^2\pi^2 - 2\pi imat} \right), \tag{5.61}$$

as $m \to \infty$.

As $m \to \infty$ we have that

$$\frac{e^{-2m\pi} + 1}{e^{-2m\pi} e^{im \log 4} + 1} \sim 1 \tag{5.62}$$

and

$$(a^2 + b^2)t^2 - m^2\pi^2 - 2\pi imat \sim -m\pi(m\pi + 2iat). \tag{5.63}$$

Hence, we have the estimate of the integral over C'

$$S_h \sim -\frac{2t}{\sqrt{\pi m}} \exp(-\pi m) \Re \left(\frac{e^{i(m \log 4 + \pi/4)}}{m\pi + 2iat} \right), \tag{5.64}$$

as $m \to \infty$.

	$a=-2$			$a=0$			$a=2$		
m	$I-M_h$	R_h	S_h	$I-M_h$	R_h	S_h	$I-M_h$	R_h	S_h
1	$1.45E-2$	$-7.34E-3$	$9.57E-3$	$1.54E-1$	$1.51E-1$	$8.78E-3$	$-2.33E-1$	$-2.28E-1$	$-2.87E-3$
2	$2.44E-4$	$5.87E-5$	$1.11E-4$	$-6.08E-3$	$-6.31E-3$	$2.17E-4$	$3.62E-1$	$3.62E-1$	$1.98E-4$
3	$-2.74E-6$	$9.6E-10$	$-3.04E-6$	$2.71E-4$	$2.72E-4$	$-1.28E-6$	$-3.53E-2$	$-3.53E-2$	$8.66E-7$
4	$-1.56E-7$	$-3.61E-10$	$-1.4E-7$	$1.28E-6$	$1.44E-6$	$-1.56E-7$	$-9.71E-4$	$-9.71E-4$	$-1.44E-7$
5	$9.75E-11$	$-2.26E-13$	$5.25E-10$	$-4.96E-7$	$-4.94E-7$	$-6.62E-10$	$-6.6E-3$	$-6.6E-3$	$-1.77E-9$
6	$1.58E-10$	$2.16E-14$	$1.55E-10$	$-2.05E-8$	$-2.06E-8$	$1.51E-10$	$8.32E-3$	$8.32E-3$	$1.34E-10$
7	$2.11E-12$	$-1.57E-16$	$1.72E-12$	$-5.23E-10$	$-5.26E-10$	$2.65E-12$	$-3.92E-3$	$-3.92E-3$	$3.4E-12$
8	$-1.61E-13$	$1.24E-19$	$-1.64E-13$	$-1.27E-11$	$-1.26E-11$	$-1.49E-13$	$-9.27E-5$	$-9.27E-5$	$-1.26E-13$
9	$-4.77E-15$	$3.4E-21$	$-4.64E-15$	$-5.41E-13$	$-5.35E-13$	$-5.37E-15$	$6.59E-4$	$6.59E-4$	$-5.88E-15$
10	$2.36E-16$	$-4.04E-25$	$1.52E-16$	$-3.95E-14$	$-3.93E-14$	$1.26E-16$	$5.18E-5$	$5.18E-5$	$9.6E-17$

Table 5.1: The error $I - M_h$ and contribution from residues R_h and saddle points S_h for the integral $I = C_0(a, 1, 1), a = -2, 0, 2$ (as defined in equation (4.9)).

5.3.5 Discussion

In this section we evaluate numerically the discretisation error $I - M_h$ for a range of h. This allows us to compare the discretisation error with the contribution R_h from the poles and with the contribution S_h from the saddle points.

To evaluate $I = C_0(a, b, t)$ we use equation (4.15). To evaluate M_h we sum the series (5.13) for sufficiently high values of n. Taking $n = 4m^2$ proved to be sufficient. To evaluate R_h we use the exact representation (5.25), while to estimate S_h we use (5.64).

We evaluate the three quantities $I - M_h$, R_h and S_h for $m = 1, 4, \ldots 10$, $a = -2, 0, 2$, $t = 1$ and $b = 1$. We present the results in Table 5.1 and plot the base 10 logarithms of their magnitudes in Figure 5.2.

In the lower two graphs the lines representing the discretisation error $I - M_h$ and residue contribution R_h are indistinguishable. This is confirmed by inspecting columns 5 and 6 of Table 5.1, in the case $a = 0$, and columns 8 and 9 in the case $a = 2$. Furthermore, from columns 7 and 10 it is evident that the saddle point contribution S_h is small in comparison with R_h.

Thus, in both cases $a = 0$ and $a = 2$, we observe that the discretisation error $I - M_h$ is determined by R_h while the contribution from S_h is negligible in comparison. That is,

$$I - M_h \sim R_h, \tag{5.65}$$

as $m \longrightarrow \infty$, while S_h is negligible.

Thus, from (5.33), we have that

$$I - M_h \sim \begin{cases} C\exp\left(-2m\arctan(\frac{b}{a})\right), & a > 0, \\ C\exp\left(-m\pi\right), & a = 0, \end{cases} \tag{5.66}$$

as $m \longrightarrow \infty$.

From the top graph of Figure 5.2, we observe the error $I - M_h$ is determined by S_h while the contribution from R_h is negligible in comparison, that is,

$$I - M_h \sim S_h, \tag{5.67}$$

as $m \longrightarrow \infty$.

From (5.64), we have, in the case $a < 0$, that

$$I - M_h \sim C\exp\left(-\pi m\right), \tag{5.68}$$

as $m \longrightarrow \infty$.

Taken together with (5.66), this implies that

$$I - M_h \sim C\exp\left(-\alpha_{a,b} m\right), \tag{5.69}$$

as $m \longrightarrow \infty$, where

$$\alpha_{a,b} = 2\arctan(\frac{b}{a}), \qquad a > 0, \tag{5.70}$$

$$\alpha_{a,b} = \pi, \qquad a \leq 0. \tag{5.71}$$

This agrees with the finding of Ooura and Mori that quadrature methods applied to Fourier transforms of functions with poles in the right half plane result in slow convergence. In this case we have shown that, in fact, the rate of our method is $\exp(-2\arctan(\frac{b}{a})m)$ where the poles are located at $a \pm ib$, for $a > 0$ and $b > 0$. This compares unfavourably with the case $a \leq 0$ for which the rate of our method is $\exp(-\pi m)$.

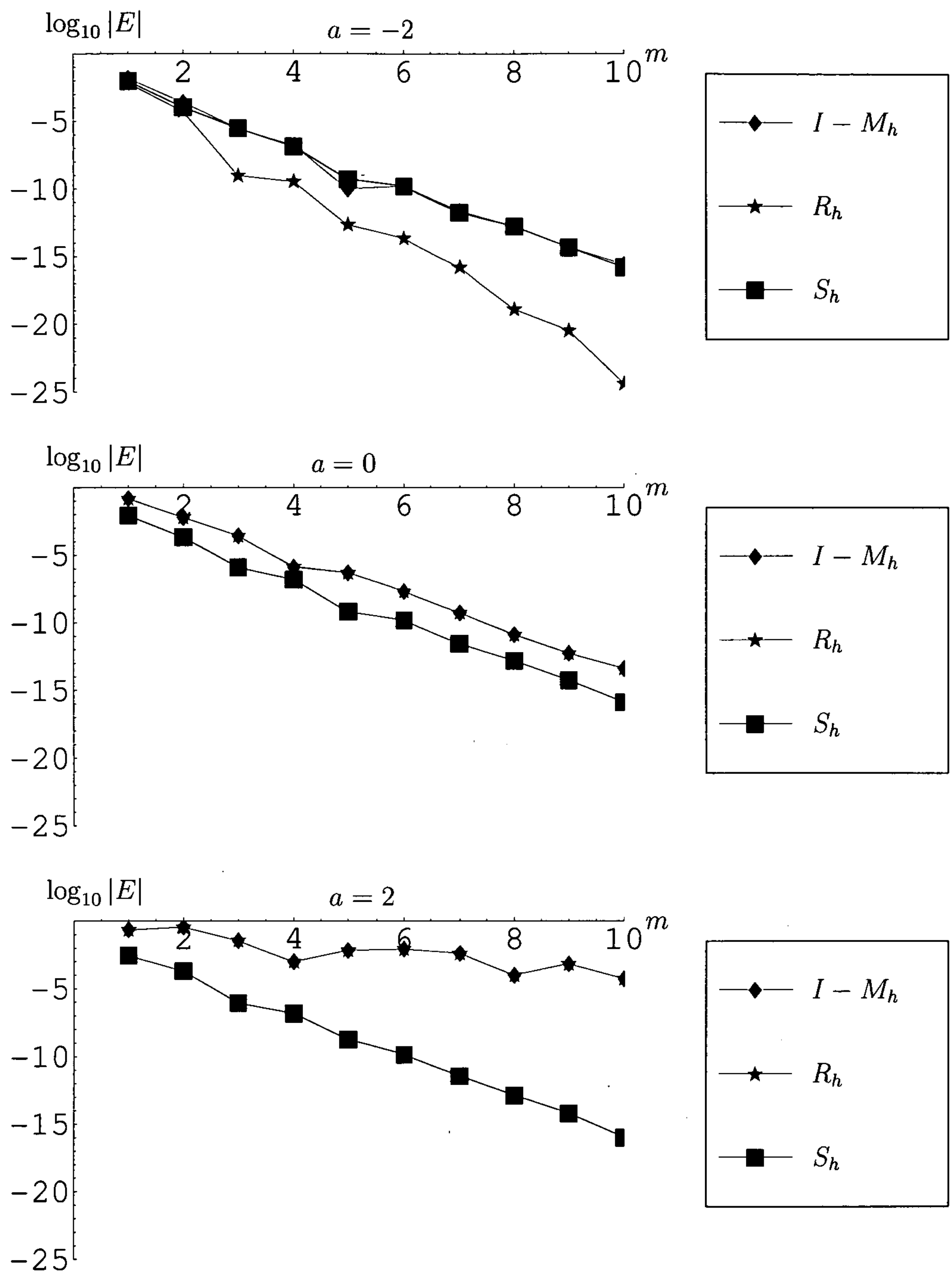

Figure 5.2: The error $I - M_h$ and contribution from residues R_h and saddle points S_h for the integral $I = C_0(a, 1, 1), a = -2, 0, 2$ (as defined in equation (4.9)).

5.4 Truncation error

We now estimate the error introduced by truncating the infinite series M_h to the finite series $M_{n,h}$, defined by

$$M_{n,h} = h \sum_{k=-n}^{n} F_m((k+1/2)h), \tag{5.72}$$

where $F_m(u)$ is given by equation (5.14). We see that the truncation error $M_h - M_{n,h}$ is bounded by

$$|M_h - M_{n,h}| \leq h \sum_{|k|>n} |F_m((k+1/2)h)|. \tag{5.73}$$

From the inequality

$$\frac{1}{(x-a)^2+b^2} \leq \frac{1}{b^2}, \tag{5.74}$$

together with equation (5.14), it follows that

$$\begin{aligned} |F_m((k+1/2)h)| &= \left| mt \frac{\cos(m\phi_3((k+1/2)h)\phi_3'((k+1/2)h)}{(\phi_3((k+1/2)h)-at)^2+b^2t^2} \right| \\ &\leq \frac{m}{tb^2} \left| \cos(m\phi_3((k+1/2)\frac{\pi}{m}))\phi_3'((k+1/2)\frac{\pi}{m}) \right|. \end{aligned} \tag{5.75}$$

Thus, to bound the truncation error we must investigate the asymptotic behaviour of $\cos(m\phi_3((k+1/2)h))$ and $\phi_3'((k+1/2)h)$ as $k \to \pm\infty$.

First, we consider the case $k \to -\infty$. Using (5.5) we have that

$$\cos(m\phi_3((k+1/2)h)) = \cos\left(me^{(k+1/2)h} + O(e^{2(k+1/2)h})\right) \tag{5.76}$$

as $k \to -\infty$. Now, using the fact that $\cos(x) = 1 + O(x^2)$ as $x \to 0$, we have that

$$\cos(m\phi_3((k+1/2)h)) = 1 + O(e^{2kh}), \tag{5.77}$$

as $k \to -\infty$. Also, by (5.7) it follows that

$$\phi_3'((k+1/2)h) = e^{(k+1/2)h} + O(e^{2kh}), \tag{5.78}$$

as $k \to -\infty$.

In the case $k \to \infty$ we proceed as follows. Using equation (5.6), we have that

$$\cos(m\phi_3((k+1/2)h)) = \cos\left(m(k+1/2)h + me^{-(k+1/2)h} + O(e^{-2kh})\right) \tag{5.79}$$

as $k \to \infty$. Now, recalling the relation $mh = \pi$ we have that $\cos(m(k+1/2)h) = 0$ and $\sin(m(k+1/2)h) = (-1)^k$, and hence from (5.79) we have that

$$\cos(m\phi_3((k+1/2)h)) = (-1)^{k+1} \sin\left(me^{-(k+1/2)h} + O(e^{-2kh})\right), \tag{5.80}$$

as $k \to \infty$. Using the fact that $\sin(x) = x + O(x^3)$, as $x \to 0$, we have that

$$\cos(m\phi_3((k+1/2)h)) = (-1)^{k+1} me^{-(k+1/2)h} + O(e^{-2kh}), \tag{5.81}$$

as $k \to \infty$. Also, by (5.8) we have that

$$\phi_3'((k+1/2)h) = 1 + O(e^{-kh}), \tag{5.82}$$

as $k \to \infty$.

Thus, using (5.77) and (5.78), equation (5.75) becomes

$$|F_m((k+1/2)h)| \leq \frac{m}{tb^2} e^{(k+1/2)h} + O(e^{2kh}), \tag{5.83}$$

as $k \to -\infty$, while using (5.81) and (5.82), equation (5.75) becomes

$$|F_m((k+1/2)h)| \leq \frac{m^2}{tb^2} e^{-(k+1/2)h} + O(e^{-2kh}), \tag{5.84}$$

as $k \to \infty$.

Thus, from (5.73) we have that

$$\begin{aligned} |M_h - M_{n,h}| &\leq \frac{hm}{tb^2} \sum_{k=-n-1}^{-\infty} e^{(k+1/2)h} + \frac{hm^2}{tb^2} \sum_{k=n+1}^{\infty} e^{-(k+1/2)h} \\ &\leq \frac{2hm^2}{tb^2} e^{-h/2} \frac{e^{-(n+1)h}}{1 - e^{-h}} \\ &\leq \frac{2hm^2}{tb^2} e^{-h/2} \frac{e^{-nh}}{h}. \end{aligned} \tag{5.85}$$

In equation (5.69) of the previous section, the discretisation error was given by the estimate

$$I - M_h \sim Ce^{-\alpha_{a,b} m}, \tag{5.86}$$

as $m \longrightarrow \infty$; where $\alpha_{a,b}$ is given by (5.70) - (5.71).

We want to balance the discretisation error $I - M_h$ and the truncation error $M_h - M_{n,h}$, hence, we equate the exponents in equations (5.85) and (5.86). We find

$$n\pi = m^2 \alpha_{a,b}. \tag{5.87}$$

This determines the relation between m and n necessary to ensure an optimal rate of convergence.

From (5.85), this choice results in an overall convergence rate of

$$I - M_{n,h} \sim C\sqrt{n}e^{-\sqrt{\alpha_{a,b}\pi n}}, \tag{5.88}$$

as $n \longrightarrow \infty$.

5.5 Comparison between our method and the method of Ooura and Mori

In this section we compare the method using the second transformation $\phi_2(u)$ of Ooura and Mori with that using our transformation $\phi_3(u)$. We shall compare the methods by applying them to the integral

$$I = C_0(0,1,1) = \int_0^\infty \frac{\cos x}{x^2+1}\, dx. \tag{5.89}$$

The method using ϕ_3 is implemented with the choice $n = m^2$, as outlined in the previous section. We denote this approximation by $M_{n,h}^{(3)}$.

To implement the method using Ooura and Mori's transformation ϕ_2 we follow the procedure as outlined in Section 3 of their paper [21]. We denote this approximation by $M_{n,h}^{(2)}$.

In Figure 5.3 we present the base 10 logarithm of the relative errors plotted against the number n of function evaluations. Clearly our method results in asymptotically slower convergence than their method, but the two methods are comparable for moderate values of n. In fact, both methods approximate I to an accuracy of about 10^{-12} using about 200 function evaluations.

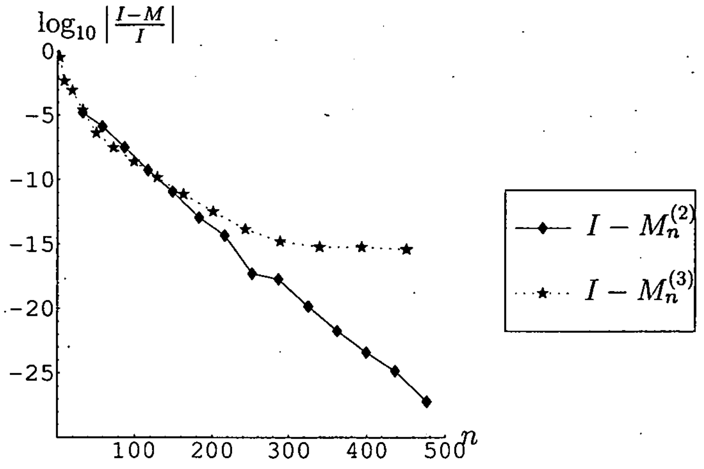

Figure 5.3: Our single exponential method ϕ_3 vs Ooura and Mori's double exponential method ϕ_2 for the oscillatory integral $C_0(0, 1, 1)$ (cf. the nonoscillatory case - Figure 3.2)

However, the number of function evaluations and error are not the only relevant considerations when comparing these methods. The cost of calculating weights and nodes must also be taken in to account. Furthermore, our transformation is much simpler in form allowing an extensive error analysis, while as we saw in Section 4.5 Ooura and Mori's error analysis is quite cumbersome.

From (5.88) we expect the error of our method to display single exponential behaviour, that is,

$$I - M_{n,h}^{(3)} = O(\exp(-\pi\sqrt{n})), \tag{5.90}$$

as $n \to \infty$. On taking logarithms this relation becomes

$$\log|I - M_{n,h}^{(3)}| = O(-\sqrt{n}), \tag{5.91}$$

which is clearly evident in Figure 5.3.

For Ooura and Mori's method we expect the error to exhibit double exponential behaviour, that is,

$$I - M_{n,h}^{(2)} = O(\exp(-\alpha\frac{n}{\log(n)})), \tag{5.92}$$

as $n \to \infty$. On taking logarithms this relation becomes

$$\log(I - M_{n,h}^{(2)}) = O(-\alpha \frac{n}{\log(n)}), \tag{5.93}$$

as $n \to \infty$. Which can be expressed as

$$\log(I - M_{n,h}^{(2)}) = o(-\alpha n), \tag{5.94}$$

as $n \to \infty$, which is clearly evident in Figure 5.3.

5.6 Reflection of pole about imaginary axis

We saw in Section 5.3.4 that the presence of poles in the right half plane results in a lower rate of exponential convergence than the presence of poles in the left half plane or on the imaginary axis. This agrees with Ooura and Mori. More generally, it is known that the effectiveness of quadrature methods is determined by the proximity of singularities of the integrand to the interval of integration.

In this section we provide a simple technique to increase the rate of convergence of our quadrature method when applied to integrands with poles in the right half plane. We consider the integral $C_0(a, b, t)$ as defined in equation (4.9) in the case $a > 0$. The integrand has poles $a \pm ib$ in the right half plane. From (5.69) we have that in this case the discretisation error is asymptotic to $\exp(-2\arctan(\frac{b}{a})m)$.

In order to approximate the integral $C_0(a, b, t)$ we first split it into two parts

$$\int_0^\infty \frac{\cos(xt)}{(x-a)^2+b^2}\,dx = \int_{-\infty}^\infty \frac{\cos(xt)}{(x-a)^2+b^2}\,dx - \int_{-\infty}^0 \frac{\cos(xt)}{(x-a)^2+b^2}\,dx. \tag{5.95}$$

In the first integral we make the change of variable $x = a + y$ and use equation (2.54) to give

$$\begin{aligned}\int_{-\infty}^\infty \frac{\cos(xt)}{(x-a)^2+b^2}\,dx &= \int_{-\infty}^\infty \frac{\cos((a+y)t)}{y^2+b^2}\,dy \\ &= \frac{\pi}{b}e^{-bt}\cos(at).\end{aligned} \tag{5.96}$$

For the second integral instead we make the change of variable $x = -y$ to give

$$\int_{-\infty}^0 \frac{\cos(xt)}{(x-a)^2+b^2}\,dx = \int_0^\infty \frac{\cos(yt)}{(y+a)^2+b^2}\,dy, \tag{5.97}$$

with poles at $-a \pm ib$. Thus, we have that

$$C_0(a,b,t) = \frac{\pi \cos a}{be^b} - C_0(-a,b,t). \tag{5.98}$$

Thus, in the case $a > 0$, we propose to apply our method of quadrature to the integral $C_0(-a,b,t)$ rather than $C_0(a,b,t)$. From (5.69) we predict that in this case the discretisation error will be behave like $\exp(-\pi m)$ or better.

With this technique in mind we have a quadrature method for the approximation of $C_0(a,b,t)$ for any $a \in \mathbb{R}$ with discretisation error of order $\exp(-\pi m)$.

5.7 New Problems

5.7.1 A new problem

A similar integral to the ones previously considered is

$$I = \int_0^\infty \frac{\cos x}{x^4+1}\,dx, \tag{5.99}$$

where the integrand has poles at $(\pm 1 \pm i)/\sqrt{2}$. This function has poles in the right half plane, therefore, by an analysis similar to that of Section 5.3 we predict that our method will result in a low rate of exponential convergence. In particular, by an analysis similar to that of Section 5.3 we obtain an estimate of the discretisation error

$$I - M_h \sim C \exp(-2\arctan(\frac{b}{a})m), \tag{5.100}$$

as $m \to \infty$, with $a = b = 1/\sqrt{2}$, that is,

$$I - M_h \sim C \exp(-\frac{\pi}{2}m), \tag{5.101}$$

as $m \to \infty$.

Furthermore, for this integral it is impossible to place the poles out of the right half plane using the technique of Section 5.6. Thus, we must be content with a low rate $e^{-\pi m/2}$ convergence compared to the rate $e^{-\pi m}$ as was achievable for $C_0(a,b,t)$.

5.7.2 A new hard problem

Consider the function g defined by

$$g(x) = \frac{1}{2i}\left[\cot(\frac{x-i}{2}) - \cot(\frac{x+i}{2})\right]. \tag{5.102}$$

The following partial fraction expansion occurs in Abramowitz and Stegun [1] as equation 4.3.91

$$\cot(z) = \frac{1}{z} + \sum_{k=1}^{\infty} \frac{2z}{z^2 - k^2\pi^2}. \tag{5.103}$$

Thus, $g(x)$ is given by

$$\begin{aligned} g(x) &= \frac{1}{2i}\left[\frac{2}{x-i} + 4\sum_{k=1}^{\infty}\frac{x-i}{(x-i)^2 - 4k^2\pi^2} - \frac{2}{x+i} - 4\sum_{k=1}^{\infty}\frac{x+i}{(x+i)^2 - 4k^2\pi^2}\right] \\ &= \sum_{k=-\infty}^{\infty}\frac{2}{(x-2k\pi)^2+1}, \end{aligned} \tag{5.104}$$

after some manipulation.

Alternatively, from (5.102) together with the identity $\cot z_1 - \cot z_2 = \frac{\sin(z_2 - z_1)}{\sin z_1 \sin z_2}$, we have that

$$g(x) = \frac{\sin i}{2i\sin(\frac{x-i}{2})\sin(\frac{x+i}{2})}. \tag{5.105}$$

Using the identity $2\sin z_1 \sin z_2 = \cos(z_1 - z_2) - \cos(z_1 + z_2)$ we have that

$$g(x) = \frac{\sinh 1}{\cosh 1 - \cos x}. \tag{5.106}$$

Thus, $g(x)$ a meromorphic function with simple poles at $2\pi k \pm i, k \in \mathbb{Z}$, furthermore, g is real and bounded on $\mathbb{R}$:

$$\frac{\sinh 1}{\cosh 1 + 1} \leq g(x) \leq \frac{\sinh 1}{\cosh 1 - 1}. \tag{5.107}$$

Thus, the function

$$f(x) = \frac{\sin x}{x} g(x) \tag{5.108}$$

has a well defined Fourier sine transform.

Since f has an infinite number of poles extending horizontally above and below the real axis there is no sector surrounding the positive real axis that is free of poles of f. Hence, the exponential methods of this thesis will fail completely for this function.

5.8 Single Exponential Transformation II

Here we propose another transformation $\phi_4(u)$. We shall introduce the function $\phi_4 : (-\infty, \infty) \to (0, \infty)$ defined by

$$\phi_4(u) = \begin{cases} \frac{u}{1-e^{-u}}, & u \neq 0 \\ 1 & u = 0 \end{cases}. \tag{5.109}$$

The derivative $\phi_4'(u)$ is given by

$$\phi_4'(u) = \begin{cases} \frac{e^u(e^u-1-u)}{(e^u-1)^2}, & u \neq 0 \\ 1/2 & u = 0 \end{cases}. \tag{5.110}$$

Recalling that $e^u > 1 + u, \quad u \neq 0$ shows that $\phi_4(u)$ is strictly increasing on $-\infty < u < \infty$.

For a nonnegative integer k the function $\phi_4(w)$ has a simple pole at $2k\pi i$ with residue $2k\pi i$.

In order to find the inverse function $w = \phi_4^{-1}(z)$, we must solve for w in the equation

$$(w - z)e^{w-z} = -ze^{-z}. \tag{5.111}$$

Thus, we have that

$$w = z + W_k(-ze^{-z}), \tag{5.112}$$

where $W(z)$ denotes the Lambert function defined by the equation

$$W(z)e^{W(z)} = z \tag{5.113}$$

and $W_k(z)$ denotes the k-th branch. For further details of the Lambert W- function see Corless et al. [7].

We do not pursue the analytical analysis of ϕ_4, instead, we present some numerical results applying the method of Section 4.4 first using ϕ_3 and then using ϕ_4.

In particular, we evaluate $I - M_{n,h}^{(3)}$ and $I - M_{n,h}^{(4)}$ where

$$I = C_0(0, 1, 1) = \int_0^\infty \frac{\cos x}{x^2 + 1}\, dx, \tag{5.114}$$

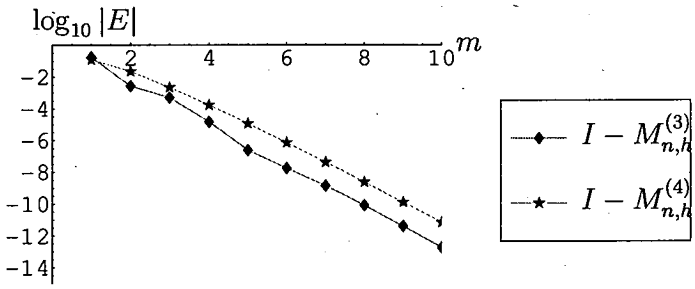

Figure 5.4: Comparison of our two single exponential methods ϕ_3 and ϕ_4 - the errors $I - M_{n,h}^{(3)}$ and $I - M_{n,h}^{(4)}$

and

$$M_{n,h}^{(j)} = h \sum_{k=-n^2}^{n^2} \frac{\cos(m\phi_j((k+1/2)h))m\phi_j'((k+1/2)h)}{(m\phi_j((k+1/2)h))^2+1}, \tag{5.115}$$

for $h = \pi/m$, $m = 1(1)10$ and $j = 3, 4$.

Both methods produce similar behaviour for this particular integral, but the analysis of ϕ_3 is easier allowing an extensive error analysis as carried out in Sections 5.2 and 5.3. However, we have included this section as the ϕ_4 is closer in form to the transformation ϕ_1 of Ooura and Mori.

Chapter 6

Linear Surface Waves II

In this chapter we return to the problem of Chapter 2.

In Section 6.1 we consider a method involving the truncation of the problem to a finite domain. This results in a problem amenable to numerical integration. However, we obtain an asymptotic estimate for the error introduced due to truncation. It is found that this error is algebraic in the point at which the truncation is made. We do not pursue this method of approximation any further, instead we use the exponential methods developed in Chapter 5.

We recall that u can be expressed as a linear combination of Fourier transforms of simple rational functions, see equation (2.47). These transforms $S_0(a, b, t)$ and $C_1(a, b, t)$ were defined in equations (2.45) and (2.46), respectively.

In Chapter 5 we developed a new single exponential method for the approximation of Fourier transforms based on a change of variable. In Section 6.2 we shall apply this new method to the approximation of S_0 and C_1. We shall see that the use of symmetry is essential.

Finally, in Section 6.3 we present graphs of the surface profile for a range of Froude numbers F.

Note that it is possible to evaluate S_0 and C_1 in terms of Si and Ci as was done for C_0 in Section 4.2. We do not do this. Instead we investigate some numerical methods for the approximation of u.

6.1 Alternative Methods Of Solution

In this section we present an alternative method of approximating the function u considered in Chapter 2. We consider a method based on domain truncation and numerical integration of the resulting initial value problem.

6.1.1 Domain Truncation

Instead of equation (2.35) with condition (2.32) consider the initial value problem

$$F^4 u_L'' + u_L = f - F^2 Hf', \qquad u_L(-L) = 0, \qquad u_L'(-L) = 0. \tag{6.1}$$

This equation can then be numerically integrated using any method for numerically solving differential equation with initial conditions such as, for example, a Runge-Kutta method. However, the error involved in approximating $u(x)$ by $u_L(x)$ is algebraic in L as we shall show.

The solution to system (6.1) is given by

$$u_L(x) = \frac{1}{F^2} \int_{-L}^{x} \sin\left(\frac{x-t}{F^2}\right) \left(f(t) - F^2 Hf'(t)\right) dt. \tag{6.2}$$

From (2.39) and (6.1) we have that

$$u(x) - u_L(x) = \frac{1}{F^2} \int_{-\infty}^{-L} \sin\left(\frac{x-t}{F^2}\right) \left(f(t) - F^2 Hf'(t)\right) dt. \tag{6.3}$$

Now, from (2.30) and (2.41) we have that

$$f(t) - F^2 Hf'(t) = -\frac{F^2-1}{\pi}\frac{1}{t^2+1} + \frac{2F^2}{\pi}\frac{1}{(t^2+1)^2} \sim -\frac{F^2-1}{\pi}\frac{1}{t^2}, \tag{6.4}$$

as $t \to \pm\infty$.

Thus, for $x \in \mathbb{R}$ we have, from (6.3) and (6.4), that

$$u(x) - u_L(x) \sim -\frac{F^2-1}{\pi F^2} \int_{-\infty}^{-L} \sin\left(\frac{x-t}{F^2}\right) \frac{1}{t^2}\, dt, \tag{6.5}$$

as $L \to \infty$. Integrating by parts gives

$$u(x) - u_L(x) \sim -\frac{F^2-1}{\pi} \left(\left[\cos\left(\frac{x-t}{F^2}\right) \frac{1}{t^2} \right]_{t=-\infty}^{t=-L} + \int_{-\infty}^{-L} \cos\left(\frac{x-t}{F^2}\right) \frac{2}{t^3}\, dt \right), \tag{6.6}$$

as $L \to \infty$. Ignoring the integral gives

$$u(x) - u_L(x) \sim -\frac{F^2 - 1}{\pi L^2} \cos\left(\frac{x + L}{F^2}\right), \tag{6.7}$$

as $L \to \infty$. Thus, we have that the maximum error $\|u - u_L\|_\infty$ behaves like

$$\|u - u_L\|_\infty = O(L^{-2}), \tag{6.8}$$

as $L \to \infty$.

This clearly demonstrates that this method of approximation is limited by this truncation error $u - u_L$ before considering the error associated with the numerical integration of the system (6.1). However, this method is quite straightforward to implement. Instead, we prefer to use the new single exponential method developed in Chapter 5 of this thesis to approximate the representation (2.47) of u involving the Fourier integrals S_0 and C_1.

6.2 Approximate evaluation of S_0 and C_1

We now apply the new method developed in Chapter 5 to the integrals $S_0(a, b, t)$ and $C_1(a, b, t)$. From equation (2.47) we see that the required parameters are $a = x, b = 1$ and $t = 1/F^2$.

We propose to use the transformation $x = m\phi_3(u)/t$ to convert these integrals to ones over $(-\infty, \infty)$ and apply the trapezoidal rule in the case of S_0 and the midpoint rule in the case of C_1. The stepsize of the quadrature rule and the parameter m are chosen according to the relation $mh = \pi$.

In the case $a > 0$ we use the technique of Section 5.6 to move the poles of the integrand into the left half plane, thus ensuring that the discretisation error is $\exp(-\alpha m)$ as $m \to \infty$, where $\alpha > \pi$. Since the value of α is unknown we assume a conservative estimate of $\exp(-\pi m)$ for the discretisation error.

Furthermore, the truncation error introduced will be of the order $\exp(-nh)$ as was seen for the integral C_0 in Section 5.4. Thus, on equating exponents the estimates of the two errors we make the choice $n = m^2$. We expect an overall rate of convergence $\exp(-\pi\sqrt{n})$.

6.2.1 Use of Symmetry

We saw in Section 5.6 that the rate of convergence of our method was limited when the integrand had poles in the right half plane. Thus, in this section we derive equations relating $S_0(a,b,t)$ and $S_0(-a,b,t)$.

From the definition of S_0 (see equation (2.45)), together with (2.54) we have that

$$S_0(a,b,t) = \frac{\pi}{b} e^{-bt} \sin(at) + S_0(-a,b,t). \tag{6.9}$$

Note that, for $a > 0$, the integrand in $S_0(a,b,t)$ has poles $a \pm ib$ in the right half plane, while $S_0(-a,b,t)$ has poles $-a \pm ib$ in the left half plane.

The following Fourier sine transform is to be found in Erdélyi [11, §2.2 (15)]

$$\int_0^\infty \frac{x\sin(xy)}{x^2+a^2}\,dt = \frac{\pi}{2}e^{-ay}, \qquad a, y > 0. \tag{6.10}$$

From the definition of C_1 (see equation (2.46)) together with (6.10) we have that

$$C_1(a,b,t) = -\pi e^{-bt}\sin(at) + C_1(-a,b,t). \tag{6.11}$$

6.2.2 Approximation to u

Thus, using equations (2.47), (2.45) and (2.46), we approximate $u(x)$ by

$$\begin{aligned} &\frac{h}{\pi F^2}\sum_{k=-m^2}^{m^2} \frac{\sin(m\phi_3(kh))F^2 m\phi_3'(kh)}{(F^2 m\phi_3(kh)-x)^2+1} \\ &-\frac{h}{\pi F^2}\sum_{k=-m^2}^{m^2} \frac{(F^2 m\phi_3((k+\frac{1}{2})h)-x)\cos(m\phi_3((k+\frac{1}{2})h))F^2 m\phi_3'(((k+\frac{1}{2})h)}{(F^2 m\phi_3((k+\frac{1}{2})h)-x)^2+1}, \end{aligned} \tag{6.12}$$

in the case $x \le 0$.

While in the case $x > 0$ we use (6.9) and (6.11) and we approximate $u(x)$ by

$$\begin{aligned} &\pi e^{-1/F^2}\sin(\frac{x}{F^2}) + \frac{h}{\pi F^2}\sum_{k=-m^2}^{m^2} \frac{\sin(m\phi_3(kh))F^2 m\phi_3'(kh)}{(F^2 m\phi_3(kh)+x)^2+1} \\ &-\frac{h}{\pi F^2}\sum_{k=-m^2}^{m^2} \frac{(F^2 m\phi_3((k+\frac{1}{2})h)+x)\cos(m\phi_3((k+\frac{1}{2})h))F^2 m\phi_3'(((k+\frac{1}{2})h)}{(F^2 m\phi_3((k+\frac{1}{2})h)+x)^2+1}. \end{aligned} \tag{6.13}$$

In approximations (6.12) and (6.13) the stepsize h is chosen to be π/m for some $m > 0$. We typically take $m = 10$.

It may seem that this method is computationally expensive as for each x different weights and nodes are used in the quadrature sums (6.13) and (6.12). It remains to be seen whether there is a more efficient method of evaluating $u(x)$.

6.3 Linearised Surface Profile

From the above approximation (see equations (6.12) and (6.13)) we obtain a graphical representation of the surface profile. From (2.9), (2.27) and (2.29) we have that the surface profile is given by

$$S(x) = -\epsilon F^2 u(x) + O(\epsilon^2), \tag{6.14}$$

where ϵ is the dimensionless vortex strength (see equation (2.2)) and F is the Froude number (see equation (2.1)) .

For comparison purposes we take $\epsilon = 0.4$ and $F = 0.7$ as these values were used by Forbes in [14] to generate his Figure 5. We plot the linearised surface profile $-\epsilon F^2 u(x)$ in Figure 6.1.

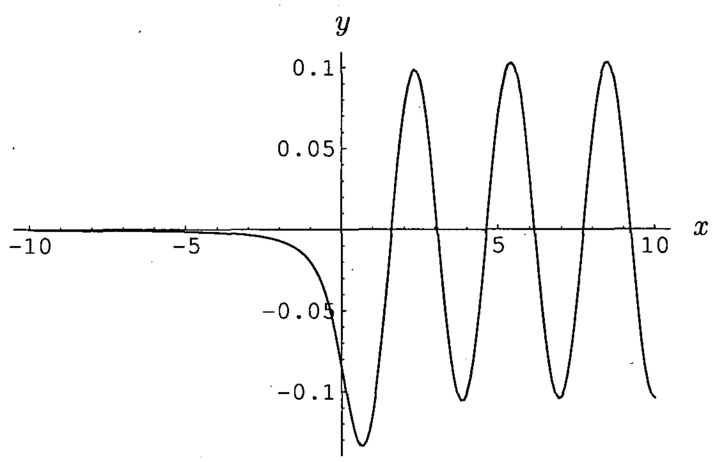

Figure 6.1: Linearised surface profile $y = -\epsilon F^2 u(x)$ for $F = 0.7$ and $\epsilon = 0.4$

Bibliography

[1] M. Abramowitz, I. A. Stegun, "Handbook of Mathematical Functions", Wiley, New York, 1972.

[2] D. E. Amos, Computation of Exponential Integrals of a Complex Argument, ACM Transactions on Mathematical Sciences, Vol. 16, No. 2, (1990) pp. 169-177.

[3] F. Bornemann, D. Laurie, S. Wagon, J. Waldvogel, "The SIAM 100-Digit Challenge: A Study in High-accuracy Numerical Computing",SIAM, Philadelphia, 2004.

[4] W. Boyce, R. DiPrima, "Elementary Differential Equations and Boundary Value Problems", Wiley, New York, 1986.

[5] R. Bracewell, "The Fourier Transform and Its Applications", McGraw-Hill Book Co., Inc., New York, N.Y., 1965.

[6] P. Butzer, R. Nessel, "Fourier Analysis and Approximation", Birkhauser Verlag, Basel, 1971.

[7] R. M. Corless, G. H. Gonnet, D. E. G. Hare, D. J. Jeffrey, D. E. Knuth, On the Lambert W-Function, Advances in Computational Mathematics, Vol. 5, (1996) pp. 329–359.

[8] P. J. Davis, P. Rabinowitz, "Methods of Numerical Integration", Academic Press, Inc., New York, N.Y., 1975.

[9] N. G. de Bruijn, "Asymptotic Methods in Analysis", North Holland, Amsterdam, 1961.

[10] J. D. Donaldson, D. Elliott, A Unified Approach To Quadrature Rules, SIAM J. Numer. Anal., Vol. 9, No. 4 (1972) pp. 573-602.

[11] A. Erdélyi et al., "Tables of Integral Transforms", Vols. 1, 2, McGraw-Hill Book Co., Inc., New York, N.Y., 1954.

[12] L.N.G. Filon, On a quadrature formula for trigonometric integrals. Proc. Roy. Soc. Edinburgh 49 (1928-29), 38.

[13] L. K. Forbes, Irregular frequencies and iterative methods in the solution of steady surface-wave problems in hydrodynamics, J. Engineering Maths., Vol. 18 (1984) pp. 299-313.

[14] L. K. Forbes, On the effects of non-linearity in free-surface flow about a submerged point vortex, J. Engineering Maths., Vol. 19 (1984) pp. 139-155.

[15] J. Lund, Sinc Function Quadrature Rules for the Fourier Integral, Math. Comp. Vol. 41, No. 163, (1983) pp. 103-113.

[16] J. Lund, K. L. Bowers, "Sinc Methods for Quadrature and Differential Equations", SIAM, Philadelphia, 1992.

[17] P. D. McLean, On a Singular Integrodifferential Equation arising from a Linearised Free Surface Problem, (In preparation).

[18] P. D. McLean, Single Exponential Approximation of Fourier Transforms, (In preparation).

[19] F. W. J. Olver, Asymptotics and Special Functions, Academic Press, New York and London, 1974.

[20] T. Ooura, M. Mori, The double exponential formula for oscillatory functions over the half infinite interval, J. Comp. Appl. Math., Vol. 38, (1991) pp. 353-360.

[21] T. Ooura, M. Mori, A robust double exponential formula for Fourier-type integrals, J. Comp. Appl. Math., Vol. 112, (1999) pp. 229-241.

[22] F. Stenger, "Numerical Methods Based on Sinc and Analytic Functions", Springer-Verlag, New York, 1993.

[23] H. Takahasi, M. Mori, Double Exponential Formulas for Numerical Integration, Publ. RIMS, Kyoto Univ., Vol. 9 (1974) pp. 721-741.